

mm Universe @ NIKA2  
Grenoble, June 05 2019

# Analysis of Galactic molecular clouds polarization maps: a review of the methods

Frédéric Poidevin



## PLAN OF TALK:

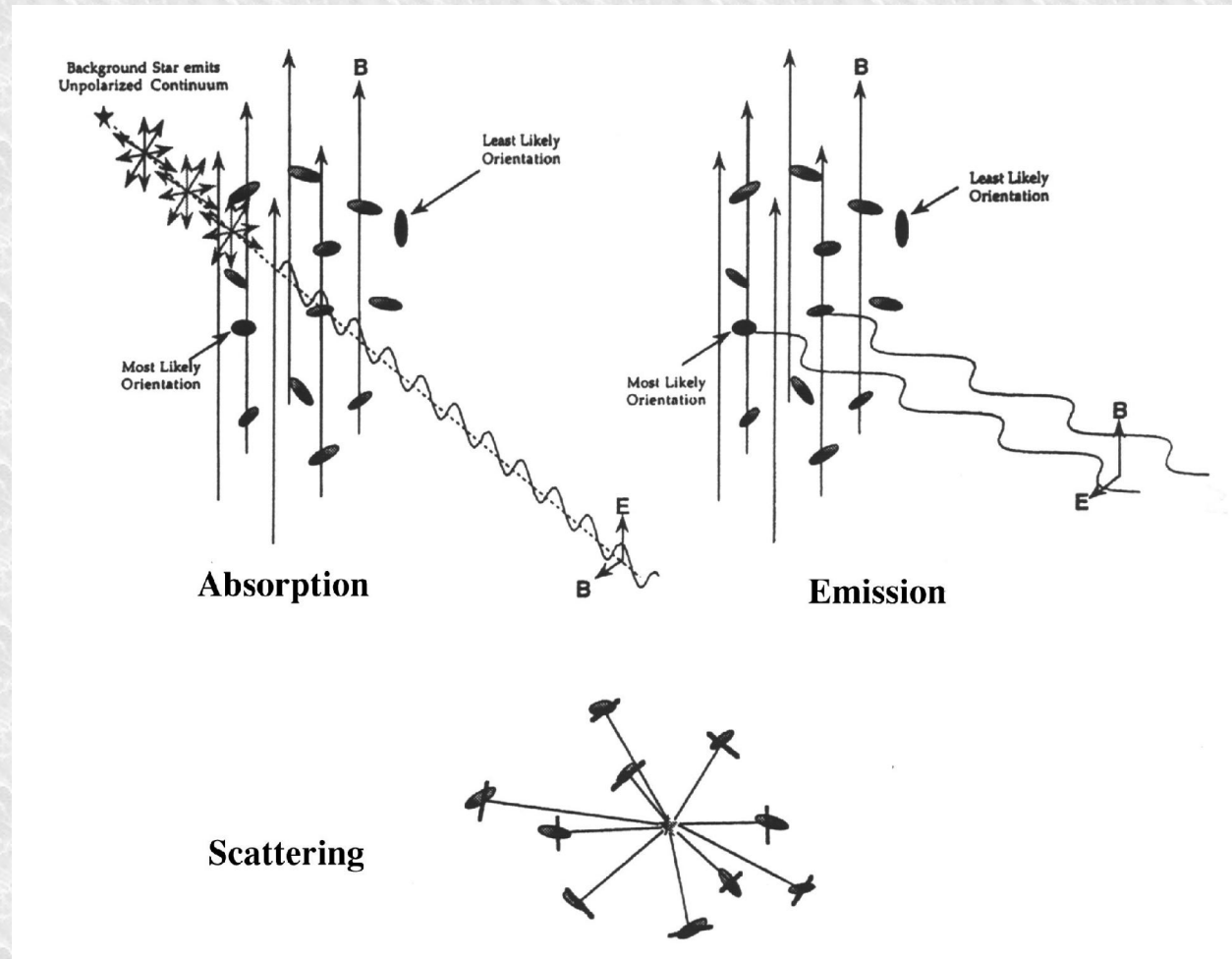
- 1) Introduction
- 2) Chandrasekhar and Fermi (CF) method and Angular Dispersion function
- 3) Histogram of Relative orientations (HROs) between column density structures and magnetic field structures
- 4) Polarization-Intensity gradient relation
- 5) Multi  $\lambda$  submm map analysis
- 6) Conclusions

## REVIEW of the methods focused on:

- Observed polarization maps
- Thermal dust emission at submm wavelengths
- Galactic studies
- Mainly molecular cloud and core scales

# 1) Introduction


## Linear polarimetry of dust grains: a probe of Magnetic Fields in the diffuse and dense ISM



Picture from **Arce et al. (1998)**

# 1) Introduction

## Molecular clouds: the coldest phase of the ISM (CMB excluded)



Component	Fractional Volume	Scale Height (pc)	Temperature (K)	Density (atoms/cm <sup>3</sup> )	State of hydrogen	Primary observational techniques
Molecular clouds	< 1%	80	10–20	10 <sup>2</sup> –10 <sup>6</sup>	molecular	Radio and infrared molecular emission and absorption lines
Cold Neutral Medium (CNM)	1–5%	100–300	50–100	20–50	neutral atomic	H I 21 cm line absorption
Warm Neutral Medium (WNM)	10–20%	300–400	6000–10000	0.2–0.5	neutral atomic	H I 21 cm line emission
Warm Ionized Medium (WIM)	20–50%	1000	8000	0.2–0.5	ionized	H $\alpha$ emission and pulsar dispersion
H II regions	< 1%	70	8000	10 <sup>2</sup> –10 <sup>4</sup>	ionized	H $\alpha$ emission and pulsar dispersion
Coronal gas Hot Ionized Medium (HIM)	30–70%	1000–3000	10 <sup>6</sup> –10 <sup>7</sup>	10 <sup>-4</sup> –10 <sup>-2</sup>	ionized (metals also highly ionized)	X-ray emission; absorption lines of highly ionized metals, primarily in the ultraviolet

Formation and evolution of Molecular Clouds in our Galaxy ?  
 Dense cold phase of the ISM where star-formation can occur :  
 $n(\text{H}) > 10^3 \text{ cm}^{-3}$  ;  $T < 100\text{K}$  ;  $M(\text{dust}) \sim 1\% M(\text{gas})$ .

Table from . See also talk by Ph. André

# 1) Introduction

## Molecular clouds formation and evolution

→ 2 main classes of models

**2 main classes of Models** for explaining the formation and evolution of such Molecular Structures :

- **Top down models** :

Investigate formation of GMCs as triggered by large scale gravitationnal, thermal and magnetic instabilities in the rotating disk of the Galaxy (e.g. Kim & Ostriker 2002)

- **Bottom-up models** :

Explore formation of GMCs by compression of substructures of the ISM by SNRs, shocks produced by superbubbles or compression in converging flows (e.g. Heitsch et al. 2009, Van Loo et al. 2007, Vásquez-Semadeni et al. 2011).

# 1) Introduction

## Star-Formation in Molecular Clouds

	Clouds <sup>a</sup>	Clumps <sup>b</sup>	Cores <sup>c</sup>
Mass ( $M_{\odot}$ )	$10^3 - 10^4$	50–500	0.5–5
Size (pc)	2–15	0.3–3	0.03–0.2
Mean density ( $\text{cm}^{-3}$ )	50–500	$10^3 - 10^4$	$10^4 - 10^5$
Velocity extent ( $\text{km s}^{-1}$ )	2–5	0.3–3	0.1–0.3
Crossing time (Myr)	2–4	$\approx 1$	0.5–1
Gas temperature (K)	$\approx 10$	10–20	8–12
Examples	Taurus, Oph, Musca	B213, L1709	L1544, L1498, B68

<sup>a</sup>Cloud masses and sizes from the extinction maps by Cambr sy (1999), velocities and temperatures from individual cloud CO studies.

<sup>b</sup>Clump properties from Loren (1989) ( $^{13}\text{CO}$  data) and Williams, de Geus & Blitz (1994) (CO data).

<sup>c</sup>Core properties from Jijina, Myers & Adams (1999), Caselli et al. (2002a), Motte, Andr  & Neri (1998), and individual studies using  $\text{NH}_3$  and  $\text{N}_2\text{H}^+$ .

Table : **Bergin and Tafalla (2007)**

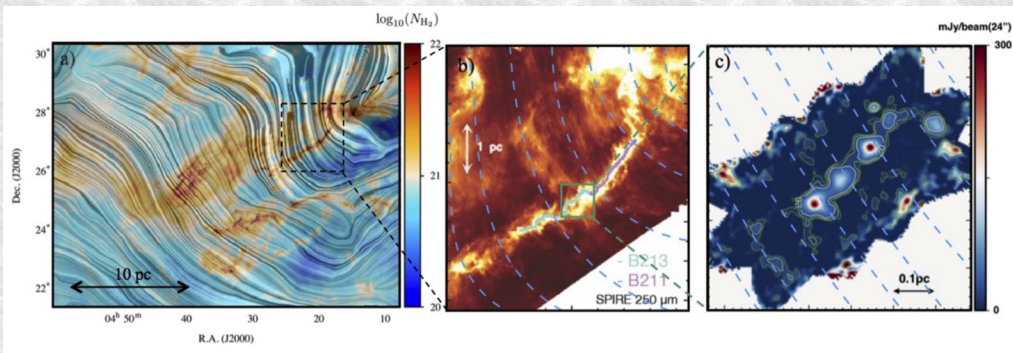
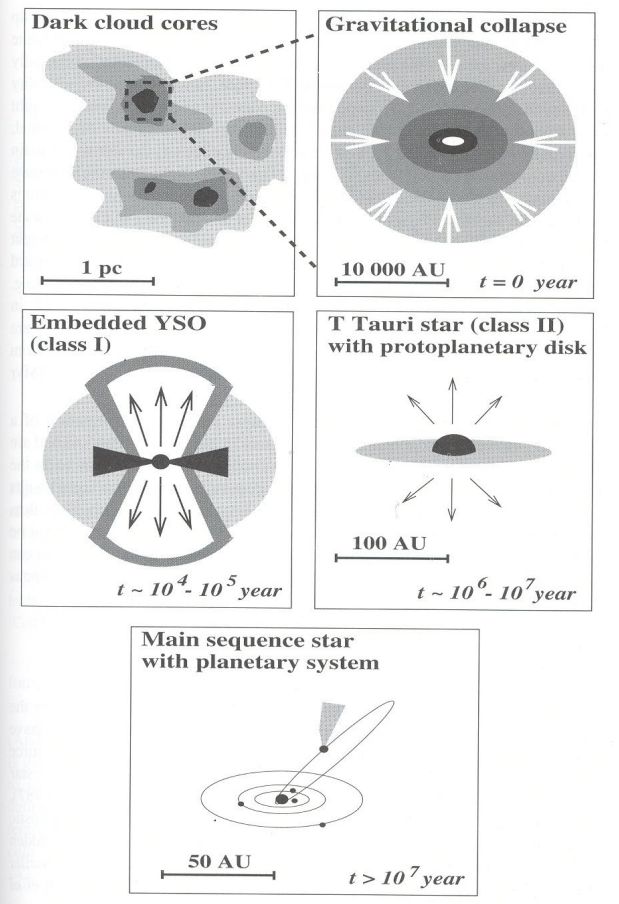


Figure : **SPICA-POL (B-BOP) article (2019)**

Fig. from **Dust in the Galactic Environment** by **DCB Whittet**.  
  IOP publishing (2003)

## 2) Chandrasekhar & Fermi (CF) method and Angular Dispersion Function

MAGNETIC FIELDS IN SPIRAL ARMS

S. CHANDRASEKHAR AND E. FERMI

University of Chicago  
*Received March 23, 1953*

POLARIZATION OF STELLAR RADIATION. III. THE POLARIZATION OF 841 STARS\*

W. A. HILTNER

Yerkes and McDonald Observatories  
*Received April 17, 1951*

Initially applied to the Galactic Disc and the diffuse ISM (1953) :

Hypothesis :

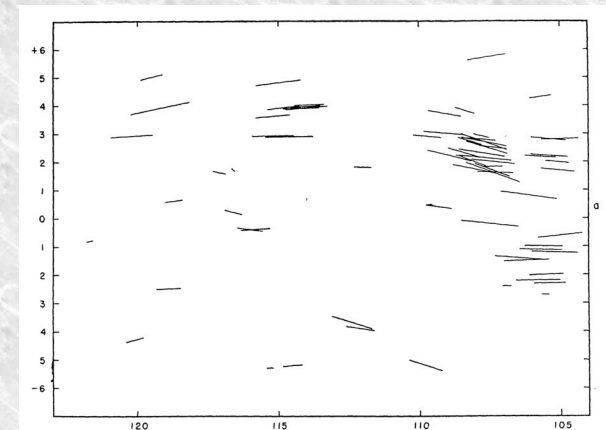
- turbulence of the ISM is isotropic
- gas coupled to Alfvénic perturbations such that there is equipartition between kinetic and perturbed magnetic energies

Dispersion of magnetic field lines based on polarized starlight - data catalog from Hiltner (1951)

$$H = \left(\frac{4}{3}\pi\rho\right)^{1/2} \frac{v}{\alpha}$$

→  $B_{\text{pos}} = 6 \mu\text{G}$  in the diffuse ISM

Example of polarization map at low Galactic latitude by Hiltner (1951) →



## 2) Chandrasekhar & Fermi (CF) method and Angular Dispersion Function

### THE FAR-INFRARED POLARIZATION OF THE ORION NEBULA<sup>1</sup>

D. P. GONATAS,<sup>2</sup> G. A. ENGARGIOLA,<sup>2</sup> R. H. HILDEBRAND,<sup>3</sup> S. R. PLATT,<sup>4</sup> AND X. D. WU<sup>4</sup>  
University of Chicago, Enrico Fermi Institute

J. A. DAVIDSON  
NASA Ames

G. NOVAK

University of Massachusetts, Amherst, Five College Radio Astronomy Observatory, and Department of Physics and Astronomy

AND

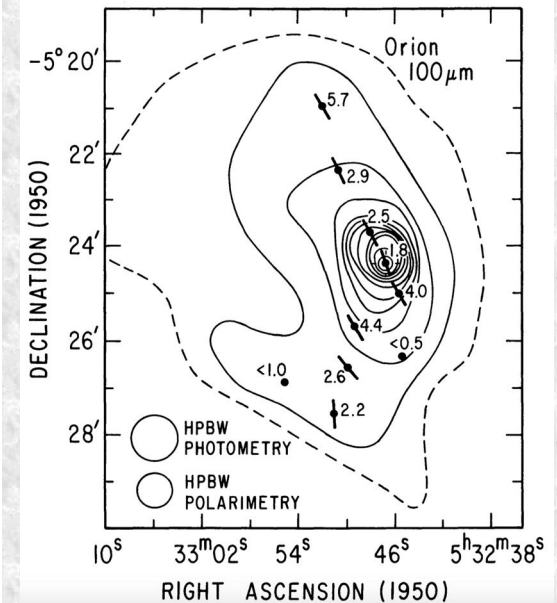
D. K. AITKEN AND C. SMITH  
Australian Defence Force Academy

Received 1989 October 30; accepted 1989 December 19

#### ABSTRACT

We have measured polarization of the 100  $\mu\text{m}$  thermal emission from 10 points in the Orion nebula. At one of the positions the degree, 5.7%, is the largest far-infrared polarization yet discovered. Except at a position in the barlike structure to the south, the position angles of the polarization vectors are well-ordered, suggesting that a uniform magnetic field threads the cloud. We estimate the magnetic field strength to be between 0.7 and 4 mG. We discuss the relationship of the degrees of polarization to the physical conditions in the cloud.

*Subject headings:* interstellar: magnetic fields — nebulae: Orion nebula — polarization



CF method transposed on spatial scales of cores and molecular clouds in denser regions of the ISM (e.g. **Gonatas et al. 1990**), i.e. on spatial scales  $\sim 1000 - 10000$  times lower than the Galactic disk.

The method was then used for analysing many submm polarization maps



## 2) Chandrasekhar & Fermi (CF) method and Angular Dispersion Function

### DISPERSION OF MAGNETIC FIELDS IN MOLECULAR CLOUDS. I

ROGER H. HILDEBRAND<sup>1,2</sup>, LARRY KIRBY<sup>1</sup>, JESSIE L. DOTSON<sup>3</sup>, MARTIN HOUDE<sup>4</sup>, AND JOHN E. VAILLANCOURT<sup>5</sup>

<sup>1</sup> Department of Astronomy and Astrophysics and Enrico Fermi Institute, The University of Chicago, Chicago, IL 60637, USA

<sup>2</sup> Department of Physics, The University of Chicago, Chicago, IL 60637, USA

<sup>3</sup> NASA Ames Research Center, Moffett Field, CA 94035, USA

<sup>4</sup> Department of Physics and Astronomy, The University of Western Ontario, London, ON N6A 3K7, Canada

<sup>5</sup> Division of Physics, Mathematics, & Astronomy, California Institute of Technology, Pasadena, CA 91125, USA

*Received 2008 November 5; accepted 2009 February 5; published 2009 April 16*

$$\langle \Delta \Phi^2(\ell) \rangle^{1/2} \equiv \left\{ \frac{1}{N(\ell)} \sum_{i=1}^{N(\ell)} [\Phi(\mathbf{x}) - \Phi(\mathbf{x} + \ell)]^2 \right\}^{1/2}$$

← The SF of the polarization angles is defined as the average of the square differences between the polarization angle measured at two points separated by a distance  $l$ .

$$\frac{\langle B_t^2 \rangle^{1/2}}{B_0} = \frac{b}{\sqrt{2 - b^2}}$$

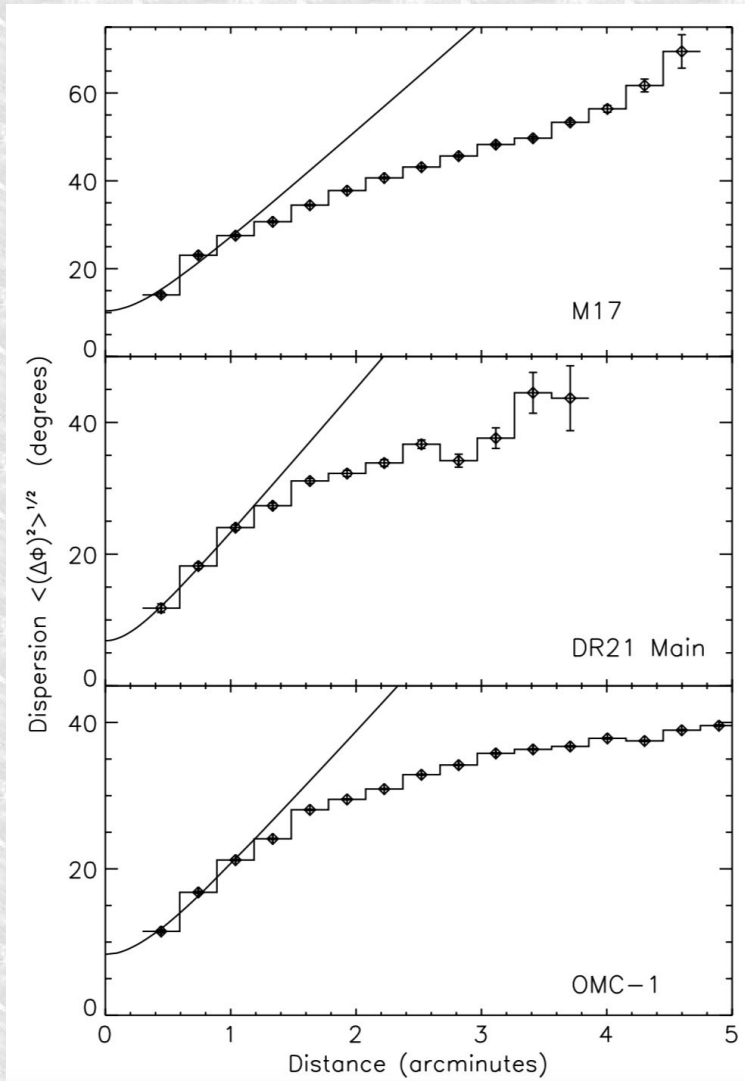
←  $B_t$  and  $B_0$  are the turbulent and uniform magnetic field components in the plane of the sky, respectively. this equation returns a direct estimate of the Turbulent-to-Mean magnetic field ratio (CF method).

$$B_0 \simeq \sqrt{(2 - b^2)4\pi\rho} \frac{\sigma(v)}{b}$$

$$\simeq \sqrt{8\pi\rho} \frac{\sigma(v)}{b},$$

← Analog to CF method adapted from the angular dispersion function

## 2) Chandrasekhar & Fermi (CF) method and Angular Dispersion Function



Results for the Dispersion, the Turbulent-to-Mean Magnetic Field Strength Ratio, the Line Widths, and the Mean Field Strength

Object	$b^a$ (deg)	$\langle B_t^2 \rangle^{1/2} / B_0^b$	$\sigma(v)$ ( $\text{km s}^{-1}$ )	$B_0^c$ (mG)
OMC-1	$8.3 \pm 0.3$	$0.10 \pm 0.01$	1.85	3.8
M17	$10.4 \pm 0.6$	$0.13 \pm 0.01$	1.66	2.9
DR21(Main)	$6.8 \pm 1.3$	$0.08 \pm 0.02$	4.09	10.6

### Notes.

<sup>a</sup> Turbulent dispersion (i.e., the dispersion limit as  $\ell \rightarrow 0$ ).

Hildebrand et al. (2009)

## 2) Chandrasekhar & Fermi (CF) method and Angular Dispersion Function

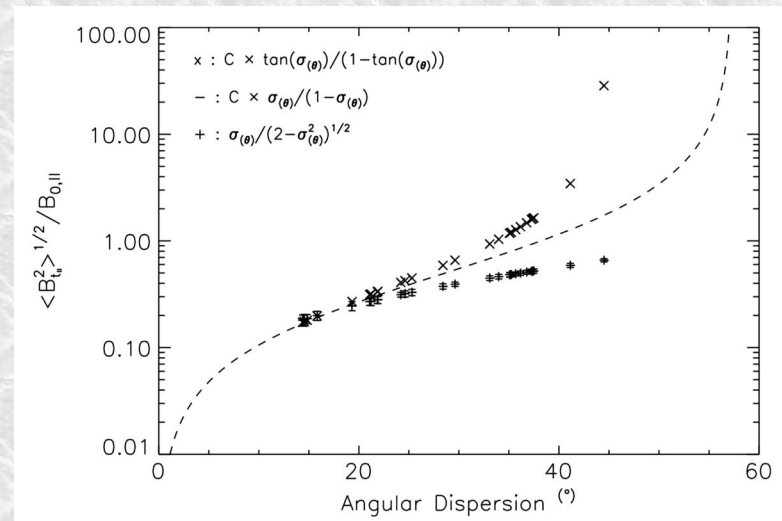
Tested with MHD simulations :

- **Ostriker et al. (2001)** : correction factor  $C \sim 0.5$
- **Falceta-Gonçalves et al. (2008)**
  - Isotropic turbulence
  - Equipartition between kinetic and mag. Energies

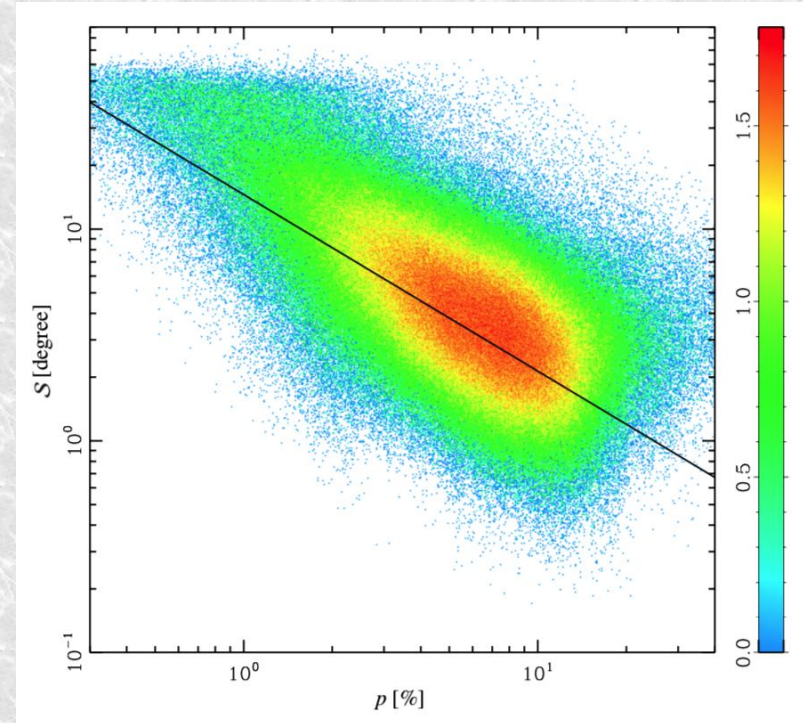
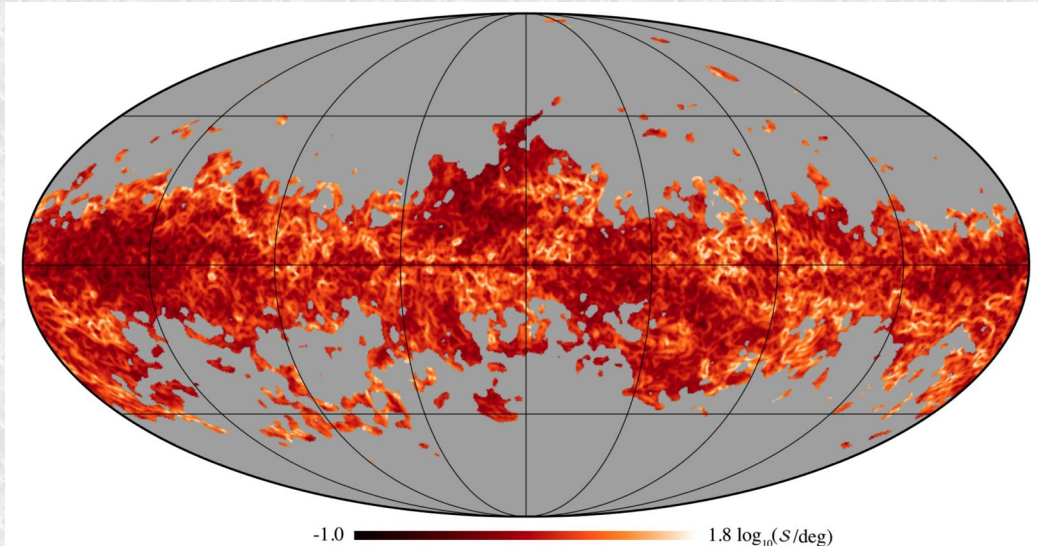
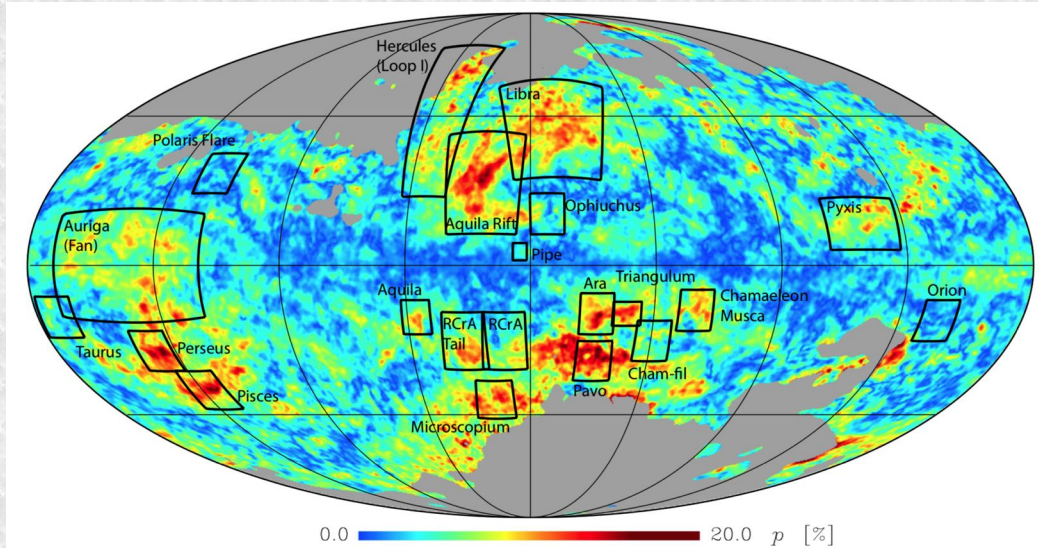
For a review on the correction factors see discussion by **Poidevin et al. (2013)**

$$B_{\text{pos}} = B_{0\parallel} + \langle B_{t\parallel}^2 \rangle^{1/2},$$

$$B_{\text{pos}} \simeq C \sqrt{4\pi\rho} \frac{\sigma(v_{\perp})}{\tan(\sigma(\theta_{\parallel}))}$$



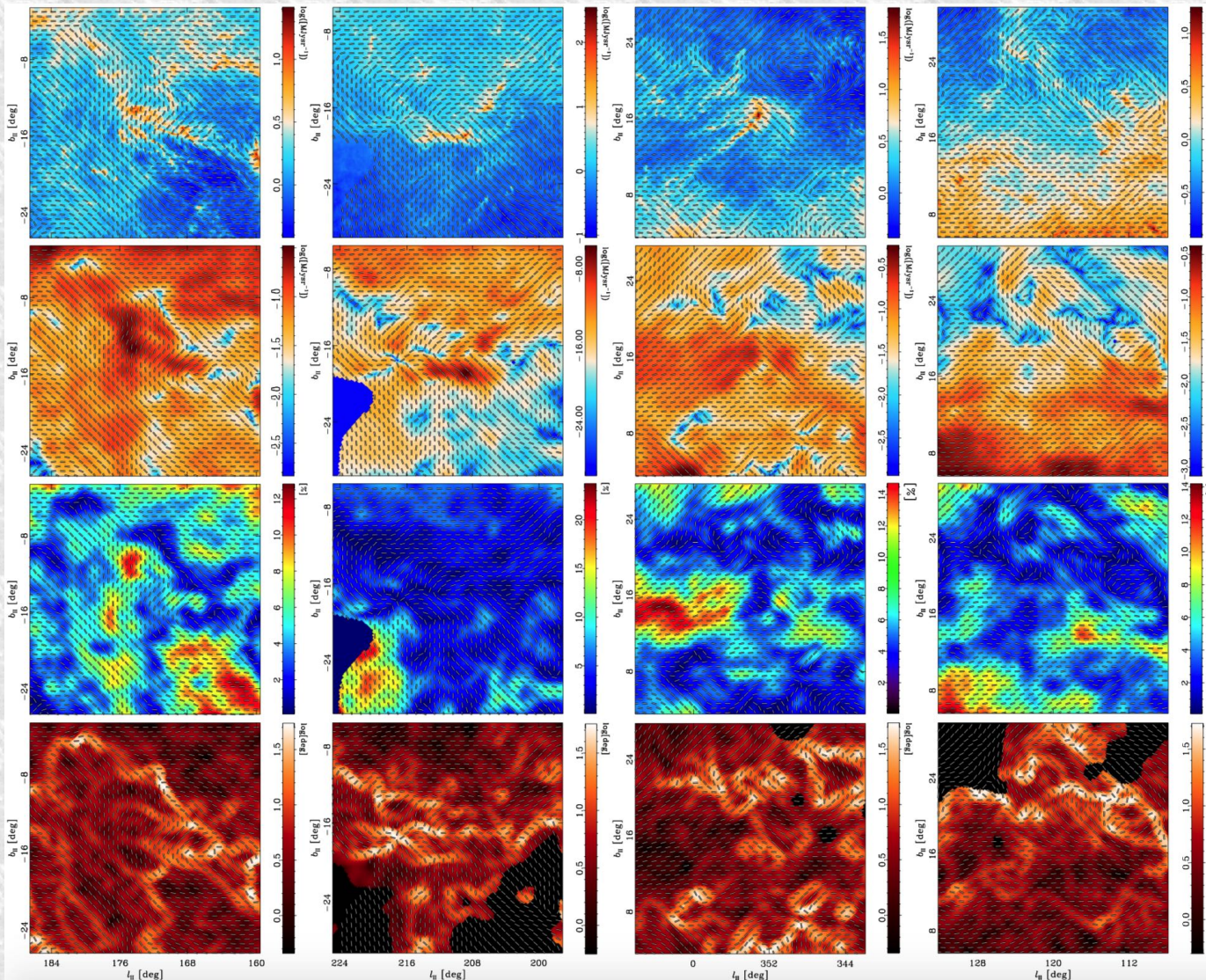
## 2) Chandrasekhar & Fermi (CF) method and Angular Dispersion Function



**Planck IR result XIX**

# 2) Chandrasekhar & Fermi (CF) method and Angular Dispersion Function

## Planck IR result XIX



Intensity

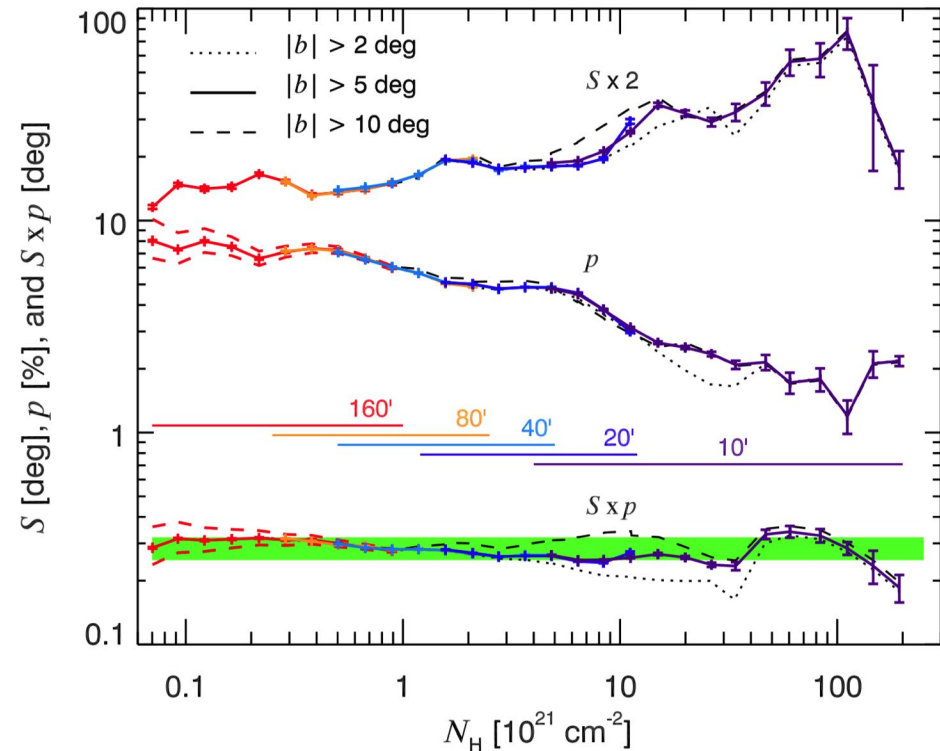
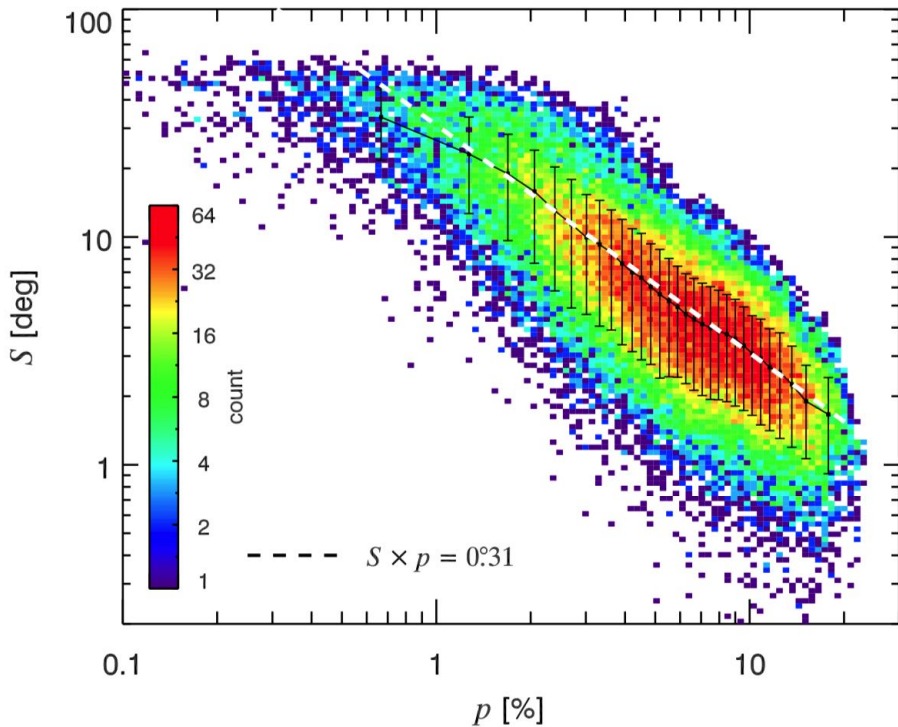
Polarized intensity

Fraction of polarization

Angular dispersion

## 2) Chandrasekhar & Fermi (CF) method and Angular Dispersion Function

### Planck 2018 XII



Two-dimensional histogram showing the joint distribution function of  $S$  and  $p$  at  $160'$  resolution, using a lag  $\delta = 80'$ . The black curve is the running mean of  $S$  as a function of the mean  $p$ , in bins of ordered  $p$ , with each bin containing the same number of pixels. The error bars represent the standard deviation of  $S$  in each bin of  $p$ . The dashed white line shows our fit  $S = 0.31/p$  to this running mean.

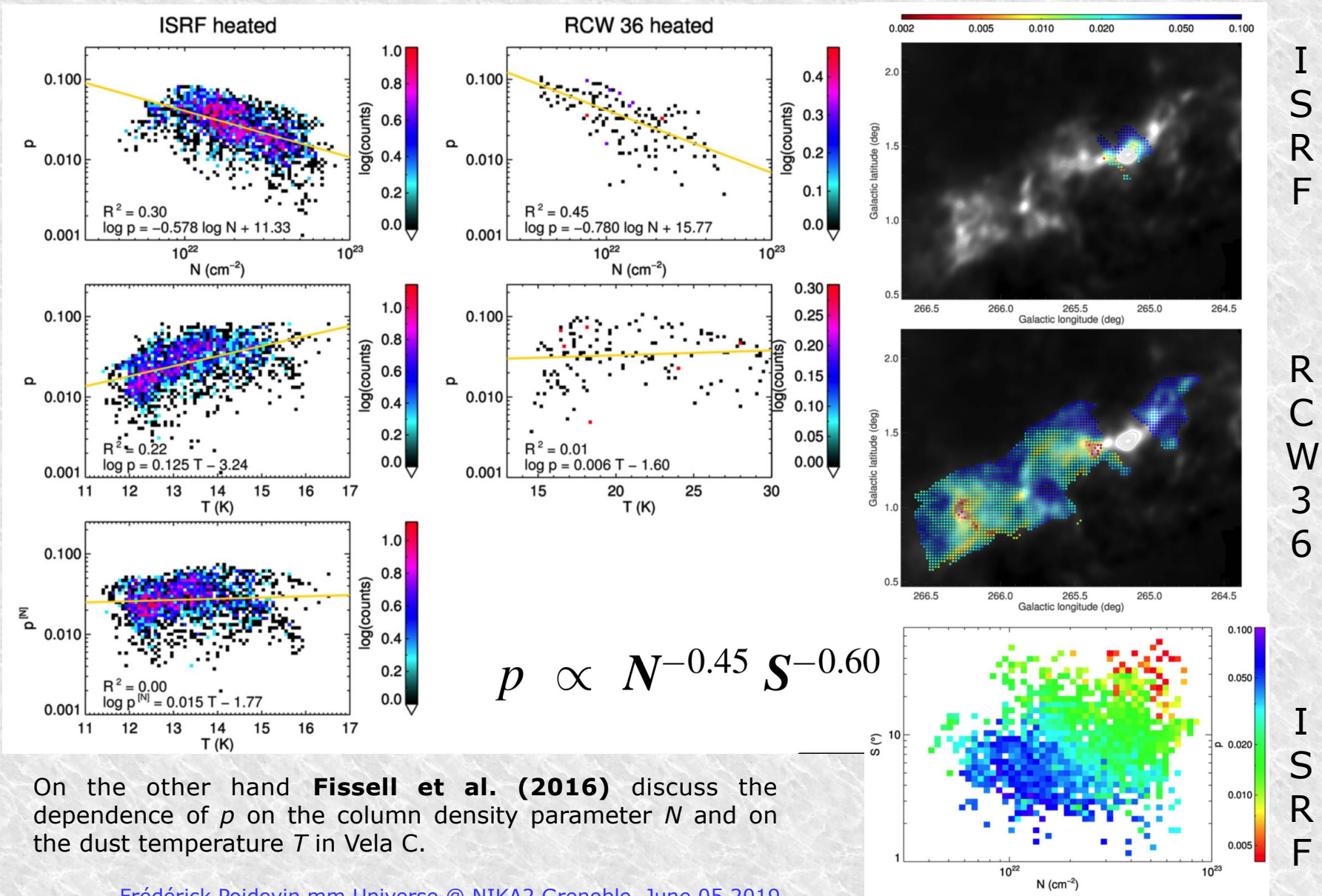
Sxp relation

$$\langle S \rangle_p = \frac{0.31}{p} \left( \frac{\omega}{160'} \right)^{0.18}$$

$\omega$ =resolution

$p$ [%] is also found to decrease with column density  $N_H$

## 2) Chandrasekhar & Fermi (CF) method and Angular Dispersion Function



On the other hand **Fissell et al. (2016)** discuss the dependence of  $p$  on the column density parameter  $N$  and on the dust temperature  $T$  in Vela C.

## 2) Chandrasekhar & Fermi (CF) method and Angular Dispersion Function

### DISPERSION OF MAGNETIC FIELDS IN MOLECULAR CLOUDS. II.

MARTIN HOUDE<sup>1</sup>, JOHN E. VAILLANCOURT<sup>2</sup>, ROGER H. HILDEBRAND<sup>3,4</sup>, SHADI CHITSAZZADEH<sup>1</sup>, AND LARRY KIRBY<sup>3</sup>

<sup>1</sup>Department of Physics and Astronomy, The University of Western Ontario, London, ON, N6A 3K7, Canada

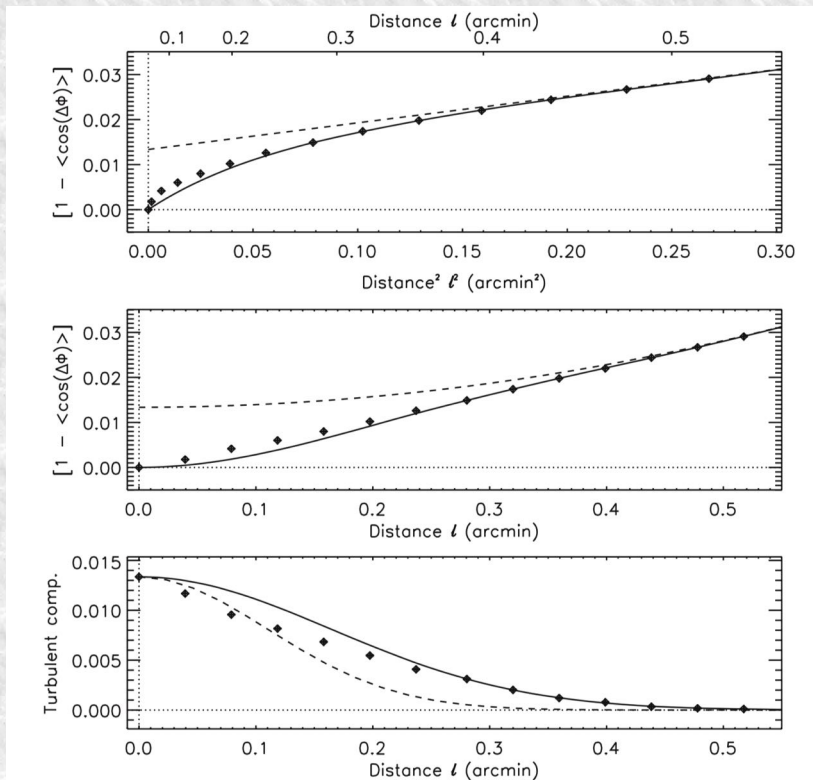
<sup>2</sup>Division of Physics, Mathematics, & Astronomy, California Institute of Technology, Pasadena, CA 91125, USA

<sup>3</sup>Department of Astronomy and Astrophysics and Enrico Fermi Institute, The University of Chicago, Chicago, IL 60637, USA

<sup>4</sup>Department of Physics, The University of Chicago, Chicago, IL 60637, USA

Received 2009 August 13; accepted 2009 September 30; published 2009 November 13

For finer analyses the area sustained by the beam + effect of the signal integration through the thickness of the cloud have to be taken into account. **Houde et al. (2009)**



Dispersion function  $1 - \langle \cos[\Delta\Phi(l)] \rangle$  for OMC-1 using the 350  $\mu\text{m}$  data obtained with SHARP.

Include the averaging of the turbulent components (Number of turbulent cells) through the column of dust.

$$1 - \langle \cos[\Delta\Phi(l)] \rangle \simeq \sqrt{2\pi} \frac{\langle B_t^2 \rangle}{\langle B_0^2 \rangle} \left[ \frac{\delta^3}{(\delta^2 + 2W^2)\Delta'} \right] \times \left[ 1 - e^{-\ell^2/2(\delta^2 + 2W^2)} \right] + a'_2 \ell^2, \quad (43)$$

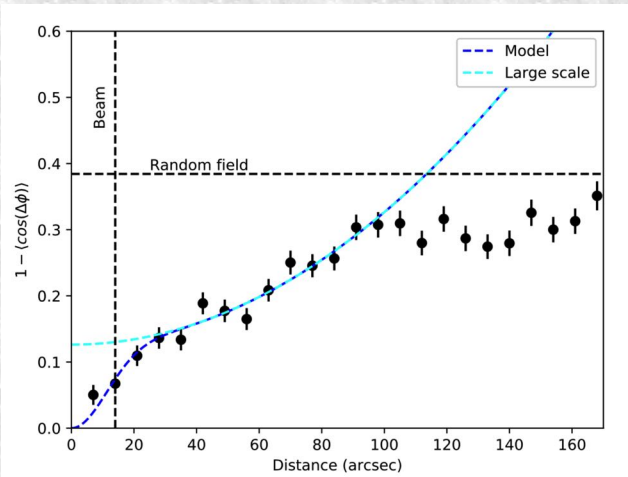
Top: fit of Equation (43) (solid curve) to the data (symbols) when plotted as a function of  $l^2$ , the broken curve does not contain the correlated part of the function (see the text)

middle: same as top but plotted as a function of  $l$ .

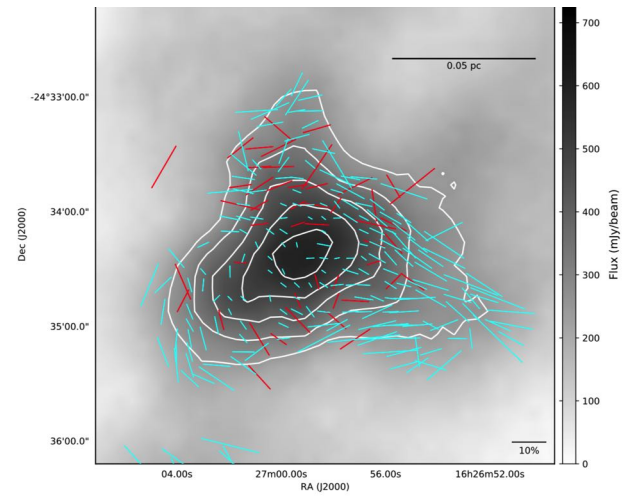
bottom: the turbulent component of the dispersion function (symbols), as obtained by subtracting the data points to the broken curve in the middle graph, while the broken and solid curves are, respectively, the contribution of the (assumed Gaussian) telescope beam alone (i.e., when  $\delta = 0$ ) and the fit to the data (i.e., with  $\delta = 7.3$ ).



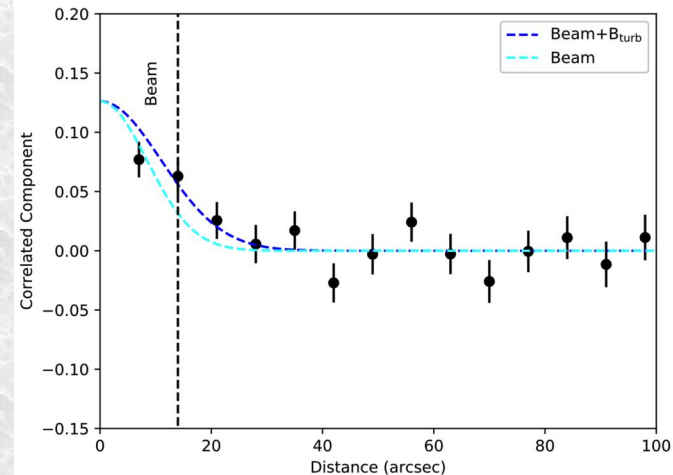
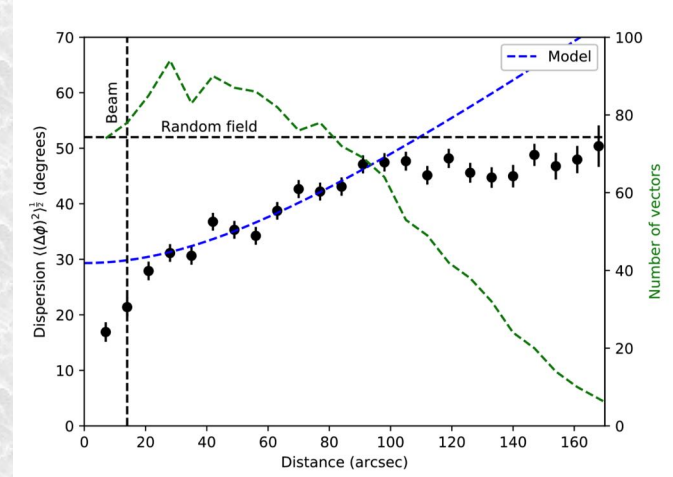
## 2) Chandrasekhar & Fermi (CF) method and Angular Dispersion Function



(a)



**Liu et al. (2019) BISTRO collaboration**  
Rho Oph with POL2 compared to SCUPOL



(b)

A blue dashed line shows the fitted dispersion function. The cyan dashed line shows the large-scale component  $(1/N)\langle\delta B_2\rangle/\langle B_0\rangle + a^2/2$  of the best fit. (b) Correlated component of the dispersion function. The correlated component  $(1/N)\langle\delta B_2\rangle/\langle B_0\rangle e^{-l^2/2(\delta^2+2W^2)}$  is shown in blue dashed line. The cyan line shows the correlated component solely due to the beam. 17

# 3) Histogram of Relative Orientations (HROs) between column density structures and magnetic field structures

## AN IMPRINT OF MOLECULAR CLOUD MAGNETIZATION IN THE MORPHOLOGY OF THE DUST POLARIZED EMISSION

J. D. SOLER<sup>1</sup>, P. HENNEBELLE<sup>2</sup>, P. G. MARTIN<sup>3</sup>, M.-A. MIVILLE-DESCHÊNES<sup>3,4</sup>, C. B. NETTERFIELD<sup>1,5</sup>, AND L. M. FISSEL<sup>1</sup>

<sup>1</sup> Department of Astronomy & Astrophysics, University of Toronto, Toronto, ON M5S 3H4, Canada; [soler@astro.utoronto.ca](mailto:soler@astro.utoronto.ca)

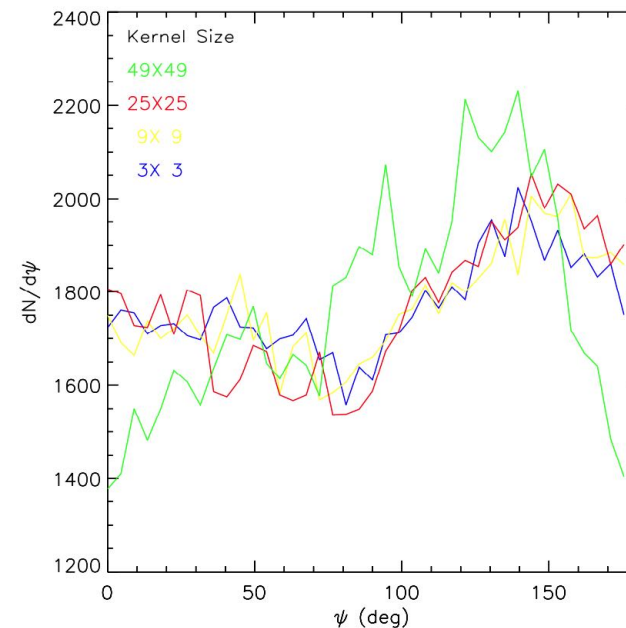
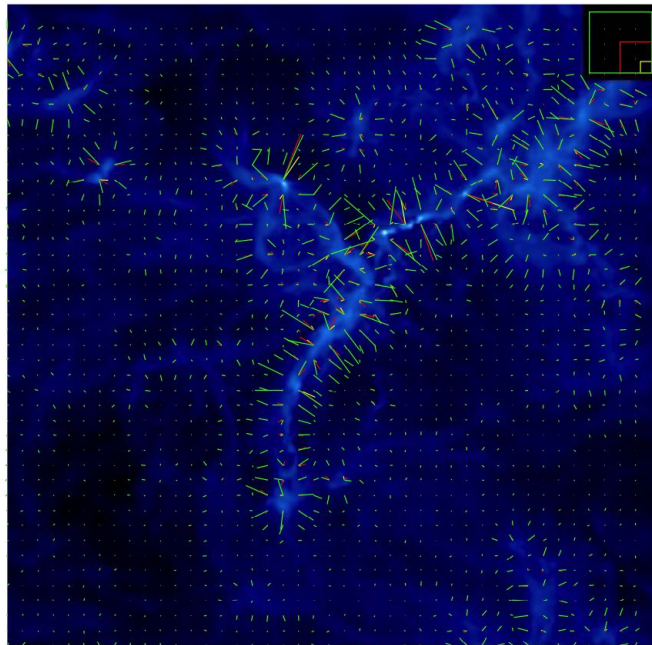
<sup>2</sup> Laboratoire de Radioastronomie, École Normale Supérieure and Observatoire de Paris, UMR CNRS 8112, 24 rue Lhomond F-75231 Paris Cedex 05, France

<sup>3</sup> Canadian Institute for Theoretical Astrophysics, University of Toronto, 60 St. George Street, Toronto, ON M5S 3H8, Canada

<sup>4</sup> Institut d'Astrophysique Spatiale CNRS, Université Paris-Sud, bâtiment 121, F-91405, Orsay, France

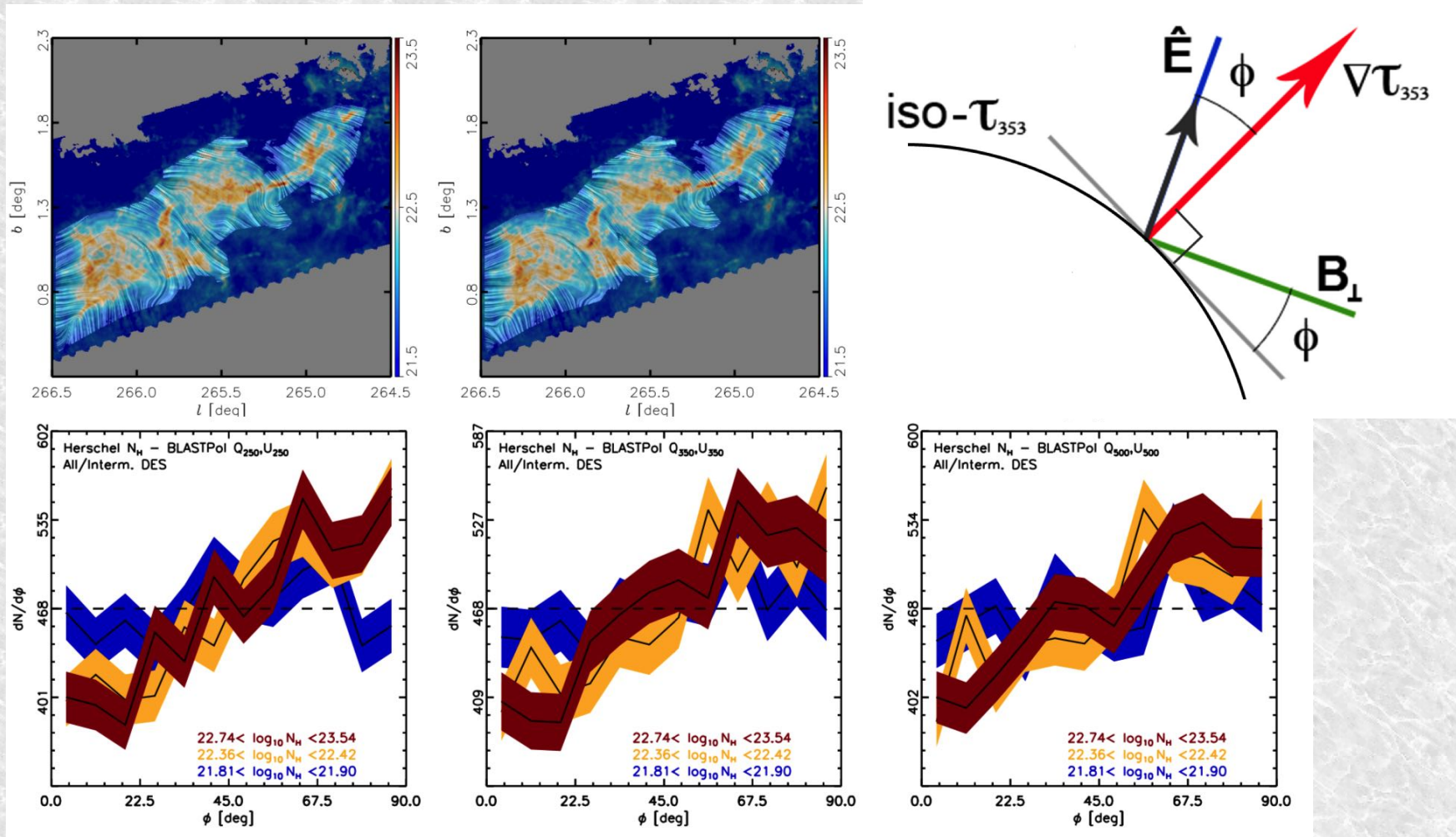
<sup>5</sup> Department of Physics, University of Toronto, 60 St. George Street, Toronto, ON M5S 1A7, Canada

Received 2013 March 5; accepted 2013 July 7; published 2013 August 23



Left: filamentary structure in the simulated column density. Overlaid are the gradient vectors obtained with derivative kernels with  $9 \times 9$  (yellow),  $25 \times 25$  (red), and  $49 \times 49$  (green) pixels. The squares on the upper right corner of the image show the sizes of these kernels. Right: histogram of orientation angles of the iso- $\Sigma$  contours ( $\psi$ ) calculated with each derivative kernel. The histograms show that the structure is predominantly oriented at  $\psi$  from  $135^\circ$  to  $150^\circ$  but also shows a secondary structure at  $45^\circ$ .

### 3) Histogram of Relative Orientations (HROs) between column density structures and magnetic field structures



**Soler et al. (2017)** – BLASTPol 250, 350, and 500  $\mu\text{m}$ , Vela C molecular ridge. 3' resolution = 0.61 pc  
 See also **Planck IR XXXV**. Probing the role of the magnetic field in the formation of structure in molecular clouds

### 3) Histogram of Relative Orientations (HROs) between column density structures and magnetic field structures

Also defined in **Soler et al. (2013)** is the histogram shape parameter  $\xi$  :

$$\xi = \frac{A_c - A_e}{A_c + A_e}$$

where  $A_c$  is the area in the centre of the histogram ( $-22^\circ.5 < \varphi < 22^\circ.5$ ) and  $A_e$  the area in the extremes of the histogram ( $-90^\circ.0 < \varphi < -67^\circ.5$  and  $67^\circ.5 < \varphi < 90^\circ.0$ ). The uncertainty is given by :

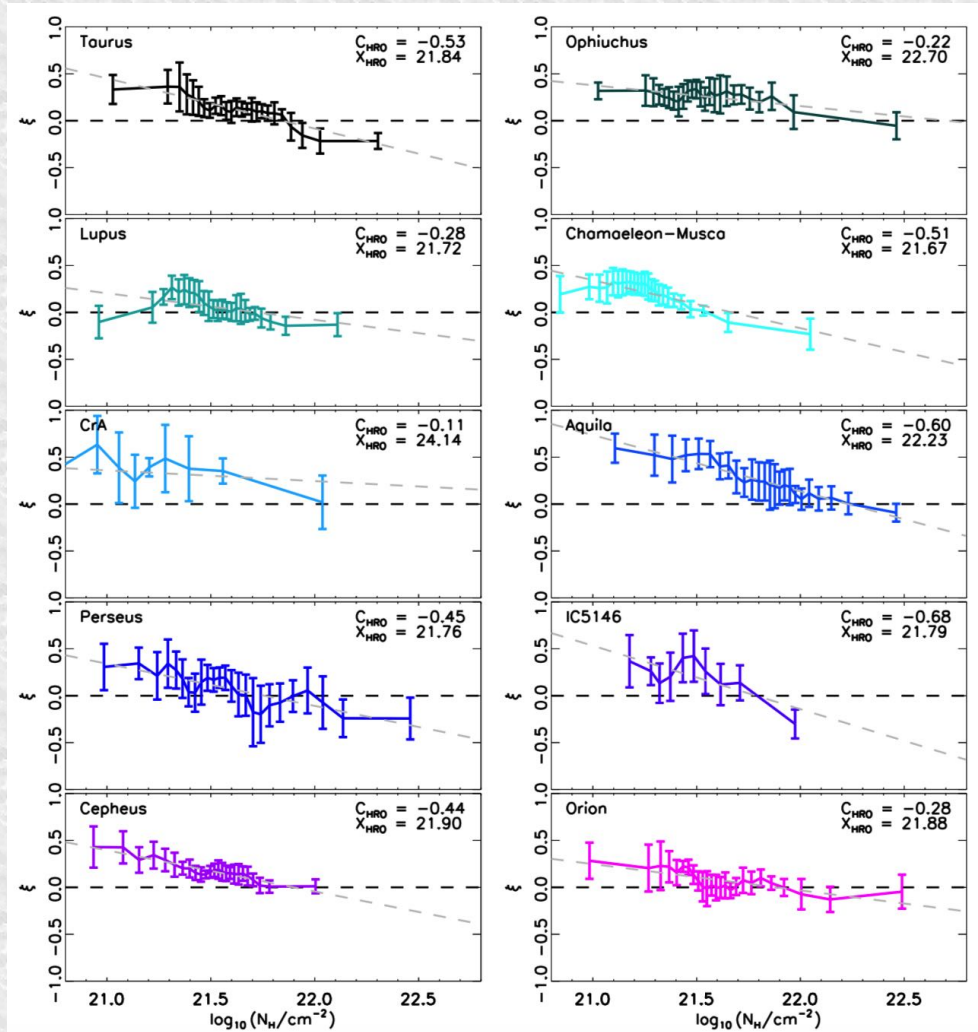
$$\sigma_\xi^2 = \frac{4 \left( A_e^2 \sigma_{A_c}^2 + A_c^2 \sigma_{A_e}^2 \right)}{(A_c + A_e)^4}$$

The trend in  $\xi$  vs.  $\log_{10}(N_H/\text{cm}^{-2})$  can be fit roughly by a linear relation :

$$\xi = C_{\text{HRO}} \left[ \log_{10} \left( N_H / \text{cm}^{-2} \right) - X_{\text{HRO}} \right]$$

For a smoother definition of  $\xi$  see **Jow et al. (2018)**

### 3) Histogram of Relative Orientations (HROs) between column density structures and magnetic field structures



Fit of  $\xi$  vs.  $\log_{10}(N_{\text{H}}/\text{cm}^{-2})$ .

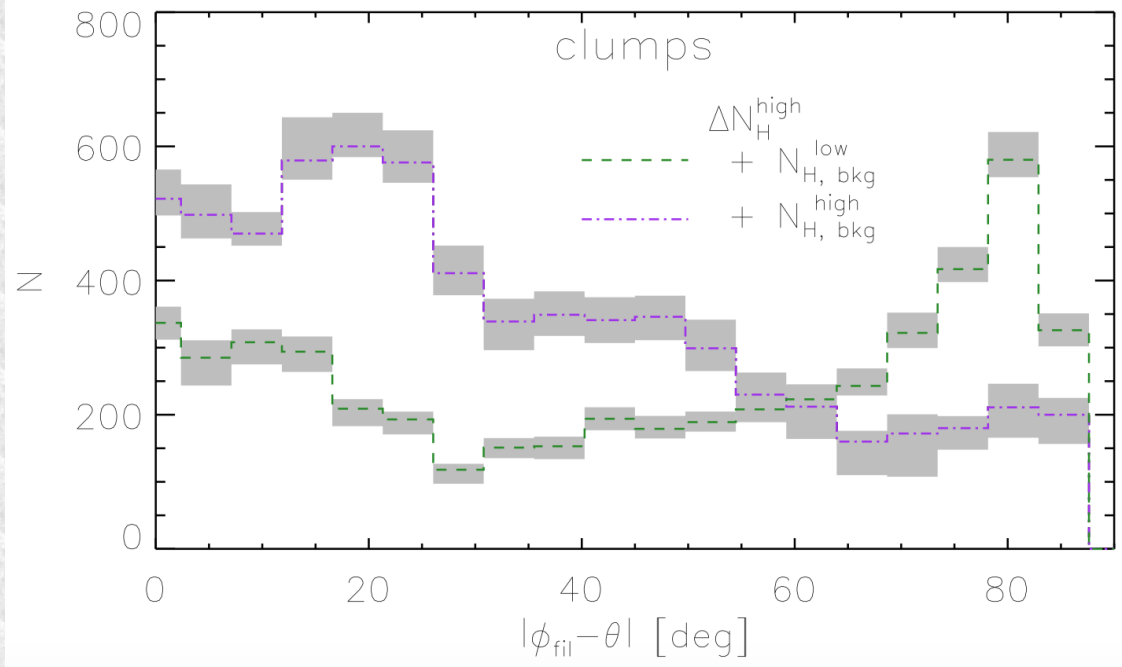
Region	$C_{\text{HRO}}$	$X_{\text{HRO}}$
Taurus	-0.53	21.84
Ophiuchus	-0.22	22.70
Lupus	-0.28	21.72
Chamaeleon-Musca	-0.51	21.67
Corona Australia (CrA)	-0.11	24.14
Aquila Rift	-0.60	22.23
Perseus	-0.45	21.76
IC 5146	-0.68	21.79
Cepheus	-0.44	21.90
Orion	-0.28	21.88

All these studies show a change of orientation from low to high density columns.

For a similar approach but with various gas density tracers see **Fissel et al. (2019)**

### 3) Histogram of Relative Orientations (HROs) between column density structures and magnetic field structures

$\Delta N_H$	Filaments	Clumps
Low	Mostly $\parallel$	Mostly $\parallel$
High	Mostly $\parallel$	$\parallel$ and $\perp$



In relation to the HRO method one can also refer to **Alina et al. (2019)** where not only the HRO is investigated but also the column density contrasts between filamentary molecular clouds and clumps. The analysis show a loss of alignment between the magnetic fields and the clumps at densities  $n_H > 10^3 \text{ cm}^{-3}$

# 4) Polarization-Intensity gradient relation

## MAGNETIC FIELD STRENGTH MAPS FOR MOLECULAR CLOUDS: A NEW METHOD BASED ON A POLARIZATION-INTENSITY GRADIENT RELATION

PATRICK M. KOCH<sup>1</sup>, YA-WEN TANG<sup>1,2,3</sup>, AND PAUL T. P. HO<sup>1,4</sup>

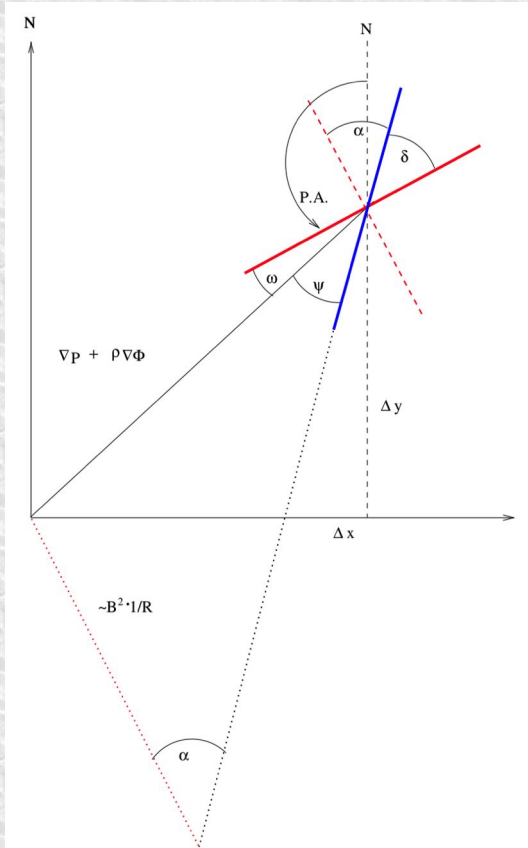
<sup>1</sup> Academia Sinica, Institute of Astronomy and Astrophysics, Taipei, Taiwan; [pmkoch@asiaa.sinica.edu.tw](mailto:pmkoch@asiaa.sinica.edu.tw)

<sup>2</sup> Observatoire Aquitain des Sciences de l'Univers, Université de Bordeaux, 2 rue de l'Observatoire, BP 89, F-33271 Floirac Cedex, France

<sup>3</sup> CNRS, UMR 5804, Laboratoire d'Astrophysique de Bordeaux, 2 rue de l'Observatoire, BP 89, F-33271 Floirac Cedex, France

<sup>4</sup> Harvard-Smithsonian Center for Astrophysics, 60 Garden Street, Cambridge, MA 02138, USA

Received 2011 March 15; accepted 2011 December 19; published 2012 February 15



Koch et al. (2012) – Assumptions of negligible viscosity and infinite conductivity (ideal MHD case) : the force equation is:

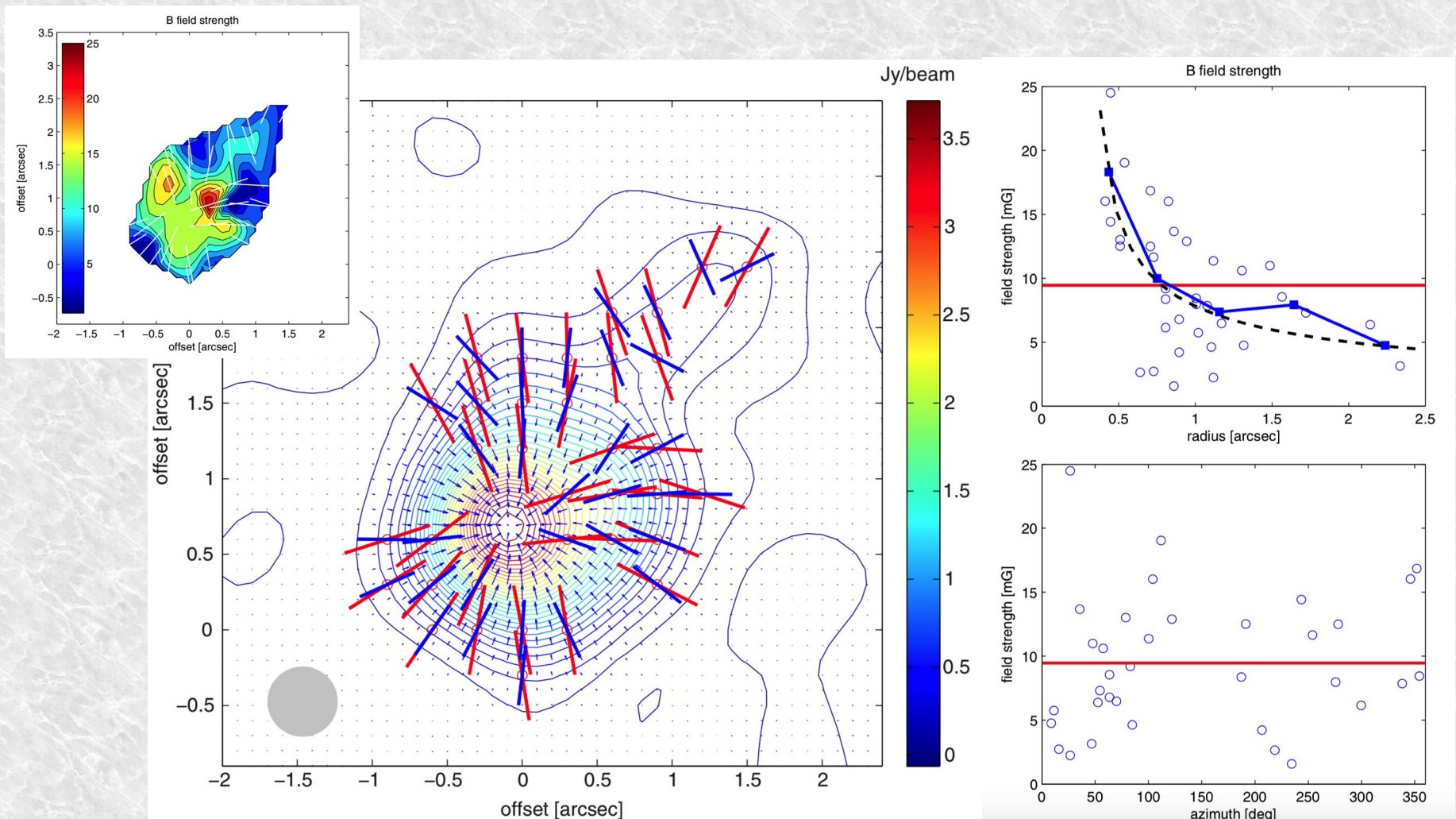
$$\rho \left( \frac{\partial}{\partial t} + \mathbf{v} \cdot \nabla \right) \mathbf{v} = -\nabla \left( P + \frac{B^2}{8\pi} \right) - \rho \nabla \phi + \frac{1}{4\pi} (\mathbf{B} \cdot \nabla) \mathbf{B}$$

$$B = \sqrt{\frac{\sin \psi}{\sin \alpha} (\nabla P + \rho \nabla \phi) 4\pi R}$$

$$\left( \frac{\sin \psi}{\sin \alpha} \right)_{\text{local}} = \left( \frac{F_B}{|F_G + F_P|} \right)_{\text{local}} \equiv \Sigma_B$$

B : mag. Field ; P : pressure ; G : Gravity

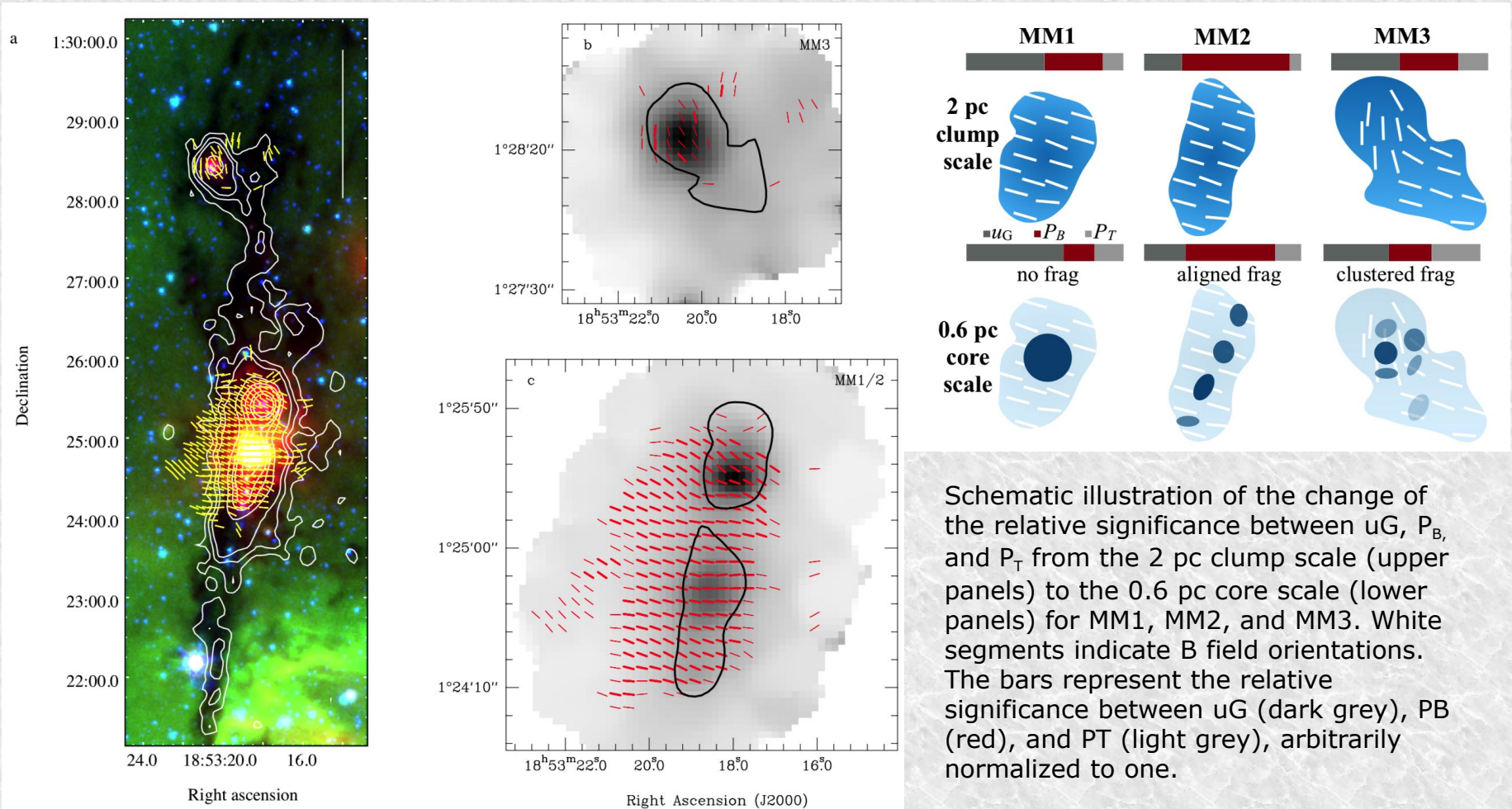
## 4) Polarization-Intensity gradient relation



**Koch et al. (2012)** : Collapsing core W51 e2 (**Tang et al. 2009**). Contours show the Stokes I dust continuum at 0.87 mm with a synthesized beam resolution of about 0.7. Overlaid are the magnetic field segments (thick red segments). The blue vector field displays the gradient directions of the dust continuum emission, with most vectors pointing toward the emission peak.



# 4) Polarization-Intensity gradient relation



Schematic illustration of the change of the relative significance between  $u_G$ ,  $P_B$ , and  $P_T$  from the 2 pc clump scale (upper panels) to the 0.6 pc core scale (lower panels) for MM1, MM2, and MM3. White segments indicate B field orientations. The bars represent the relative significance between  $u_G$  (dark grey),  $P_B$  (red), and  $P_T$  (light grey), arbitrarily normalized to one.

Very complete analysis for the case of G34 by **Tan et al. 2019** (see arxiv) where CF and angular dispersion function + polarization-intensity gradient methods are used and compared.

## 5) Multi $\lambda$ submm map analysis

### THE FAR-INFRARED POLARIZATION SPECTRUM: FIRST RESULTS AND ANALYSIS

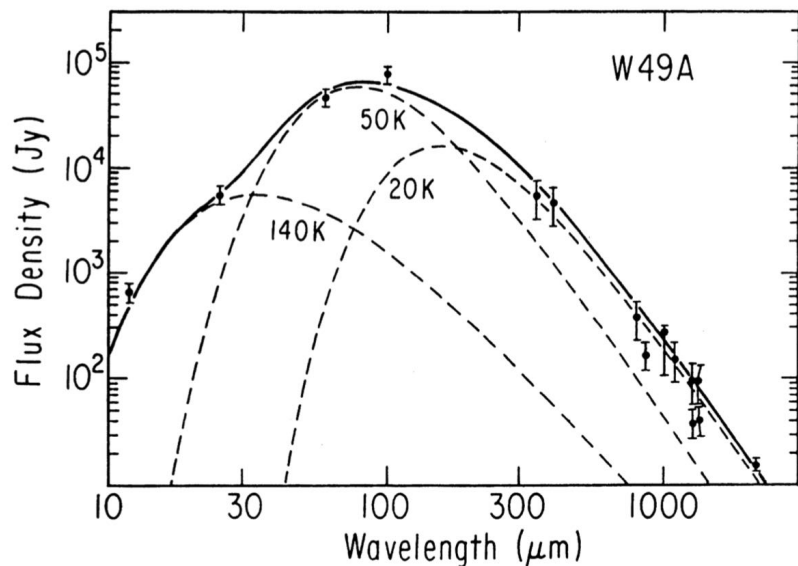
R. H. HILDEBRAND,<sup>1,2</sup> J. L. DOTSON,<sup>3</sup> C. D. DOWELL,<sup>4</sup> D. A. SCHLEUNING,<sup>1</sup> AND J. E. VAILLANCOURT<sup>1</sup>

*Received 1998 September 18; accepted 1998 December 10*

#### ABSTRACT

We present data on the polarization of the thermal emission from Galactic Clouds at 60  $\mu\text{m}$ , 100  $\mu\text{m}$ , and 350  $\mu\text{m}$ . There are examples of rising polarization spectra in dense cloud cores [ $P(350 \mu\text{m})/P(100 \mu\text{m}) \approx 2$ ], and falling spectra in cloud envelopes [ $P(350)/P(100 \mu\text{m}) \approx 0.6$ ]. We also present data showing that the relationship,  $P(\tau)$ , between polarization and optical depth in cloud cores is different from that in cloud envelopes. We review the principles governing the far-infrared polarization spectrum and discuss applications to the data on  $P(\lambda)$  and  $P(\tau)$ . We conclude that the cloud envelopes we have observed must contain two populations of grains that differ in their polarization efficiencies and in their emission spectra. We propose a model for cloud envelopes in which the contrasting populations reside in domains of different mean temperatures where the warmer domains contain the aligned grains.

*Subject headings:* dust, extinction — infrared: ISM: continuum — ISM: clouds — polarization — stars: low-mass, brown dwarfs



### A Primer on Far-Infrared Polarimetry

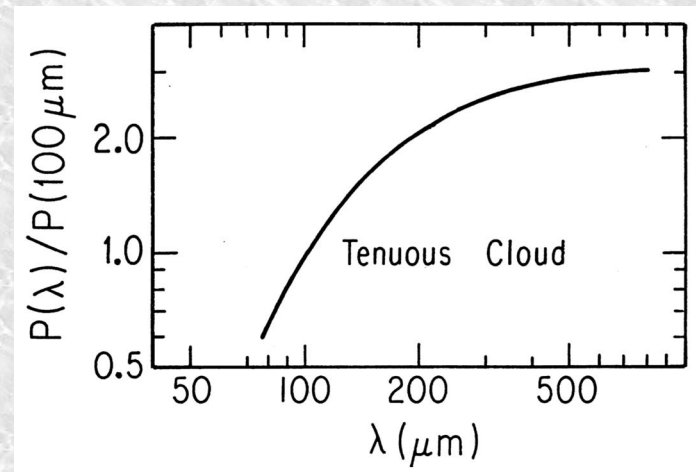
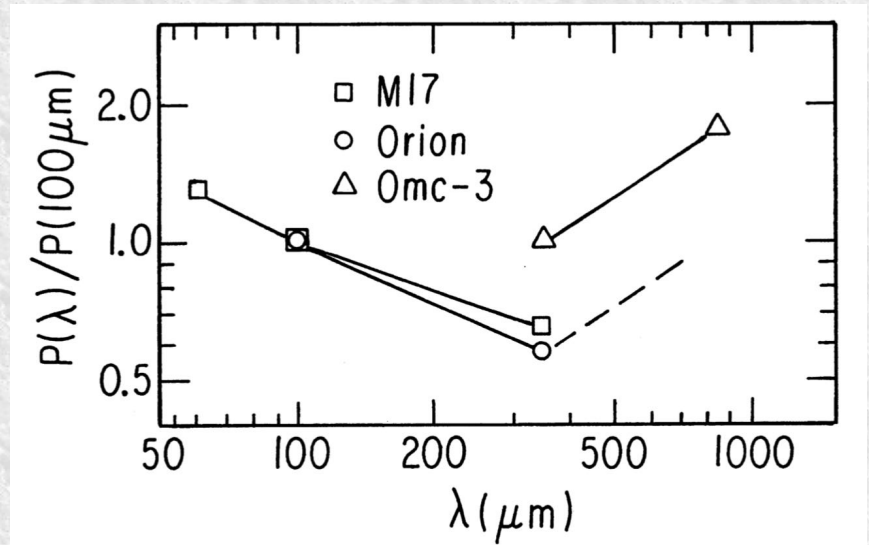
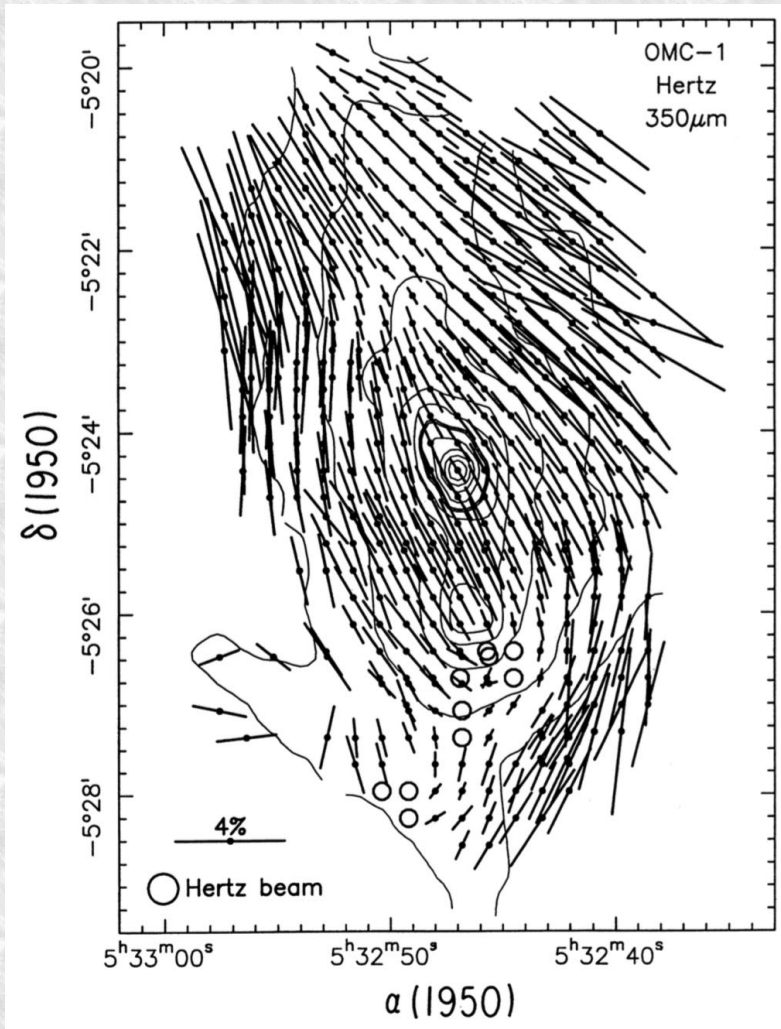
R. H. HILDEBRAND,<sup>1,2</sup> J. A. DAVIDSON,<sup>3</sup> J. L. DOTSON,<sup>4</sup> C. D. DOWELL,<sup>5</sup> G. NOVAK,<sup>6</sup> AND J. E. VAILLANCOURT<sup>1</sup>

*Received 2000 March 8; accepted 2000 April 27*

**ABSTRACT.** We present an introduction to observing procedures and principles of analysis used in far-infrared polarimetry. The observing procedures are those for single-dish observations of thermal emission from aligned dust grains. We discuss techniques for removing backgrounds and for reducing and evaluating errors. The principles of analysis are those required for interpreting polarization maps and polarization spectra in terms of opacity, field structure, and variations in temperature and polarizing efficiency.

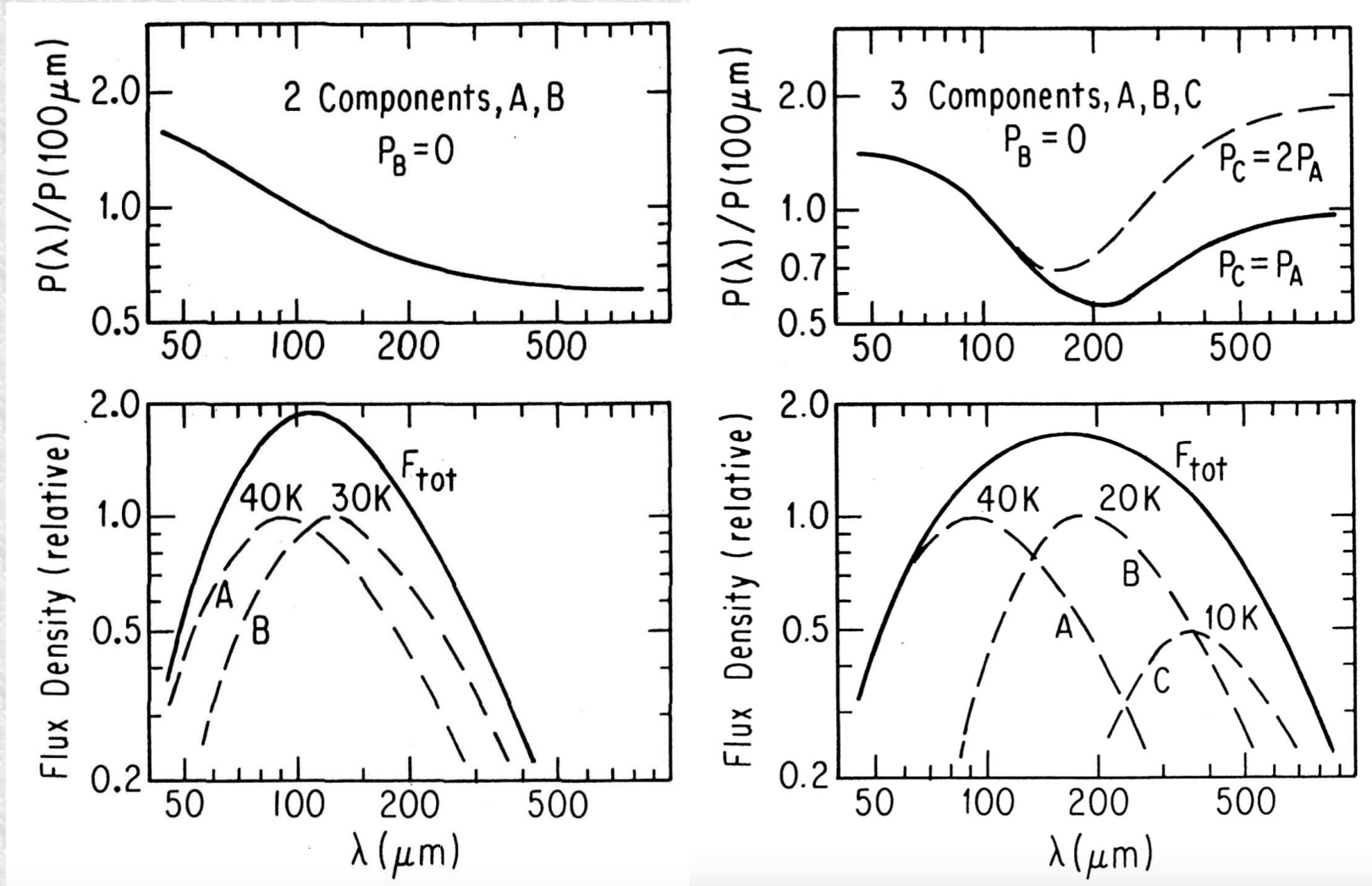
← Total flux spectrum and derived temperature components of the molecular cloud W49A. Adapted from **Sievers et al. (1991)**. (Area sampled includes warm component in core.)

## 5) Multi $\lambda$ submm map analysis



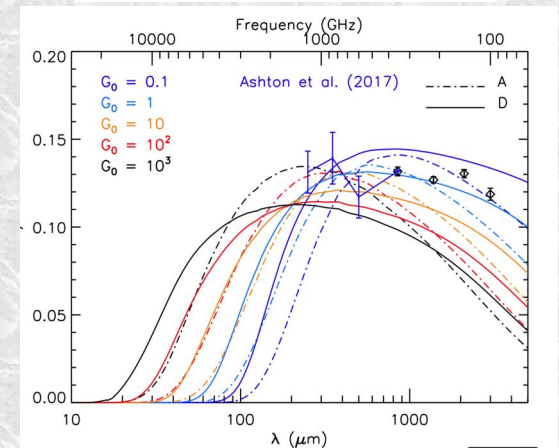
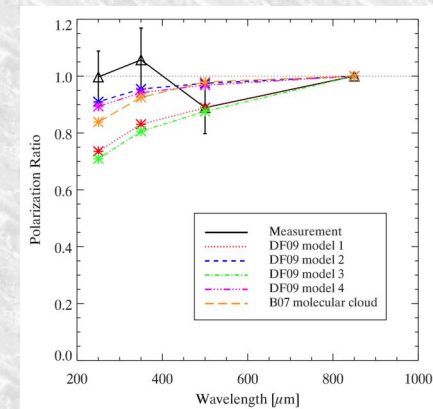
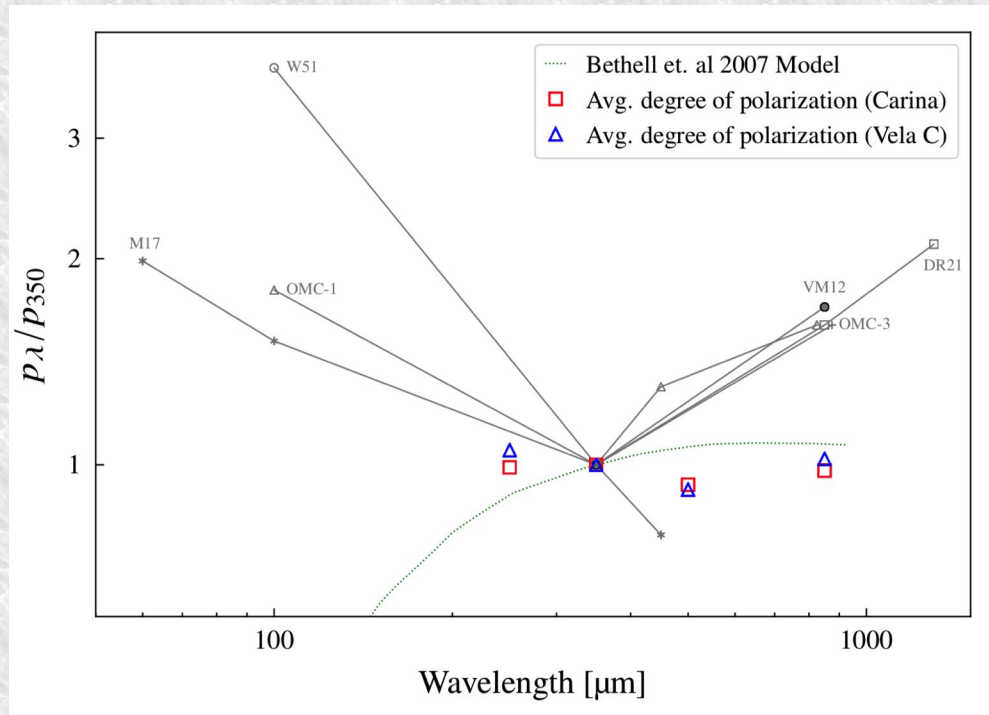
**Hildebrand et al. (2000).** Combining data obtained at different wavelengths (e.g. left figure) one can probe polarization spectra (upper right figure). A simple cloud can not reproduce the polarization spectra shape. Assume suprathermal rotation of magnetic grains.

## 5) Multi $\lambda$ submm map analysis



**Hildebrand et al. (2000)**. Left: 2 dust component model with different temperatures. Right: 3 dust components model with different temperatures can reproduce polarization spectra shape. Fit with two dust grain populations with different polarization Properties also possible as shown and discussed by **Vaillancourt et al. (2002)**. See also **Vaillancourt and Matthews (2012)** where JCMT and CSO polarimetry data are combined and compared.

# 5) Multi $\lambda$ submm map analysis



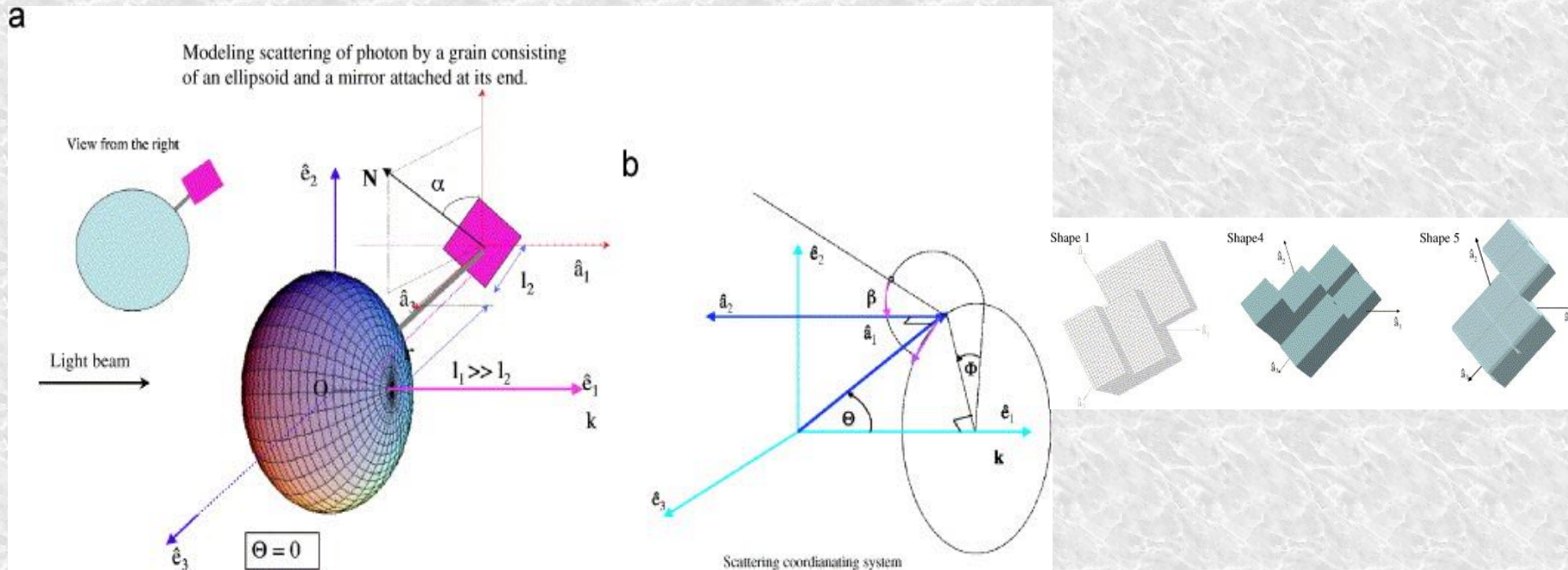
Comparison of quartiles in 850  $\mu\text{m}$  intensity in  $\text{MJy sr}^{-1}$  between *Planck* measurements and ground-based measurements of molecular clouds. The Carina Nebula values are computed over the sightlines passing the data cuts for the case of diffuse emission subtraction using the Far reference region.

	1 <sup>st</sup> Quartile	Median	3 <sup>rd</sup> Quartile
Translucent Cloud (Ashton et al. 2018)	3.1	3.4	4.1
Vela C (Gandilo et al. 2016)	6.5	9.1	14.1
Carina Nebula (this work)	7.6	10.8	17.6
Ground-based, 17 molecular clouds (Vaillancourt & Matthews 2012)	300	637	1327

BLASTPol 250, 350 and 500  $\mu\text{m}$  combined with Planck 850  $\mu\text{m}$  (353 GHz).  
 Model by **Guillet et al. (2018)** reproduce flat polarization spectrum in translucent cloud

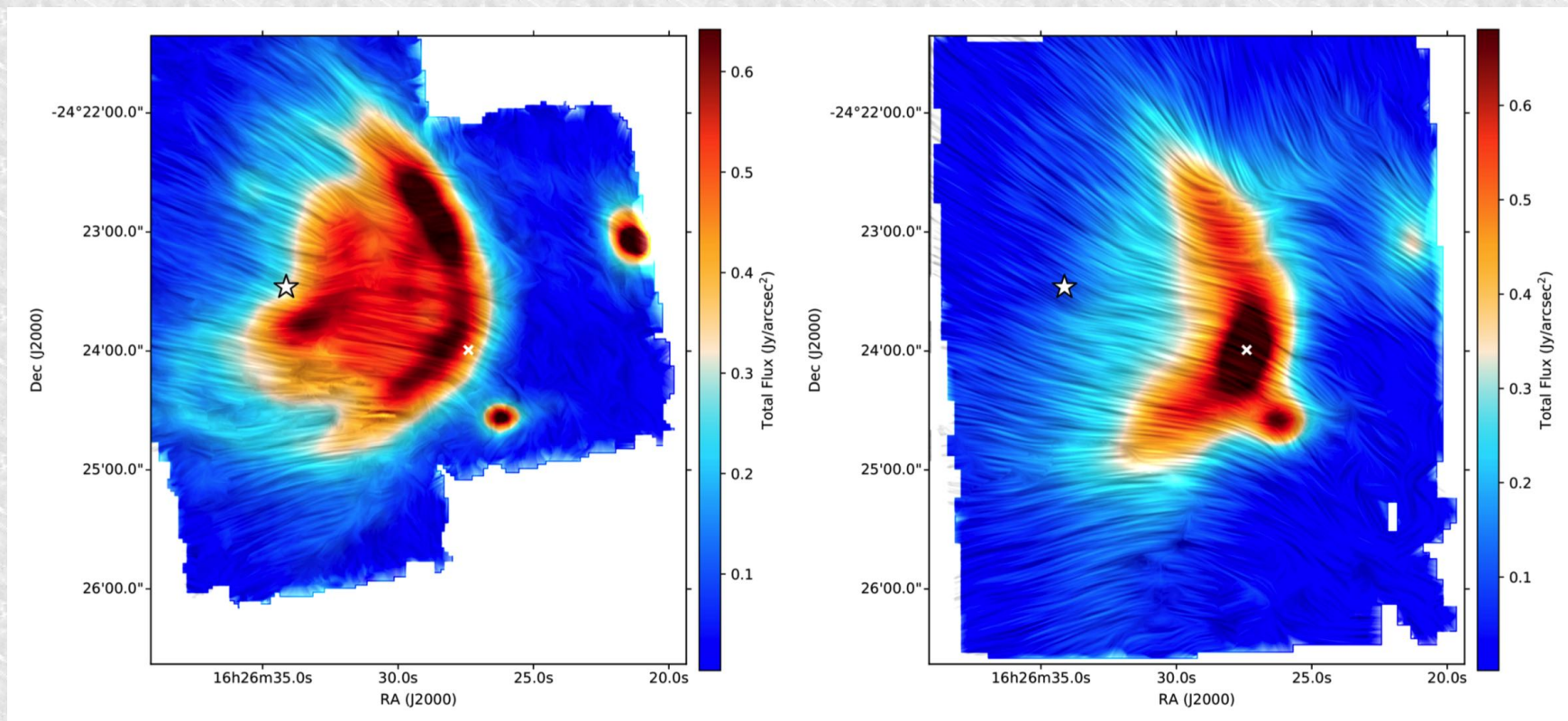
## 5) Multi $\lambda$ submm map analysis

### *DUST GRAIN ALIGNMENT BY THE ISRF AND MAGNETIC FIELDS IN THE ISM*



Current paradigm: dust grains with 'elliptical' shape are aligned by the interstellar radiation field (and will relax with short axis preferentially aligned with local B-field). See **Hoang and Lazarian works** based on first ideas proposed by **Dolginov & Mytrophanov (1976)**.

## 5) Multi $\lambda$ submm map analysis



**Santos et al. (2019):** HAWC+/SOFIA toward  $\rho$  Oph A -bands C (89  $\mu\text{m}$ ) and D (154  $\mu\text{m}$ ).  $RDC = pD/pC \rightarrow$  clear correlation between RDC and the molecular hydrogen column density across the cloud.  $RDC > 1$  dominates the lower density and well illuminated portions of the cloud, that are heated by the high mass star Oph S1.  $RDC < 1$  is observed toward the denser and less evenly illuminated cloud core. (1) Warm grains at the cloud outskirts, are efficiently aligned by the abundant exposure to radiation from Oph S1, as proposed in the radiative torques theory; (2) Cold grains deep in the cloud core, are poorly aligned due to shielding from external radiation.

## 6) Conclusions

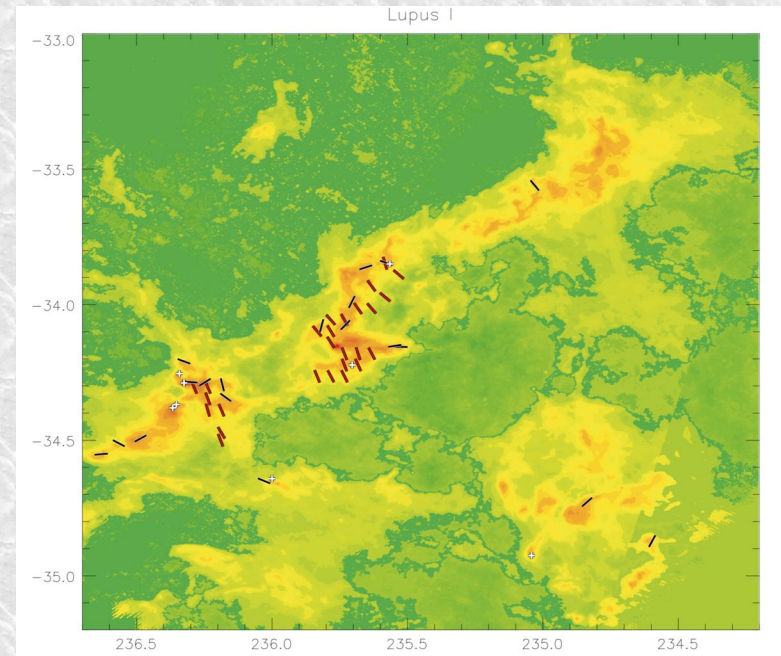
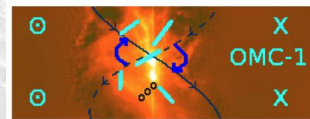
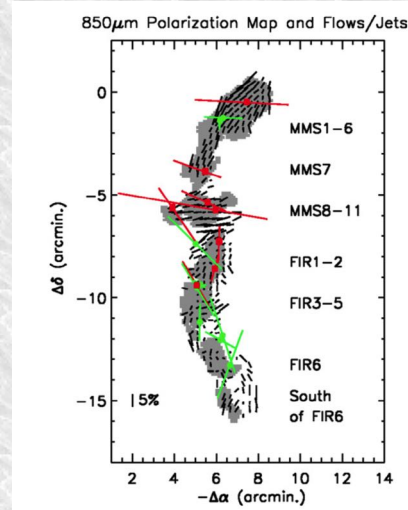
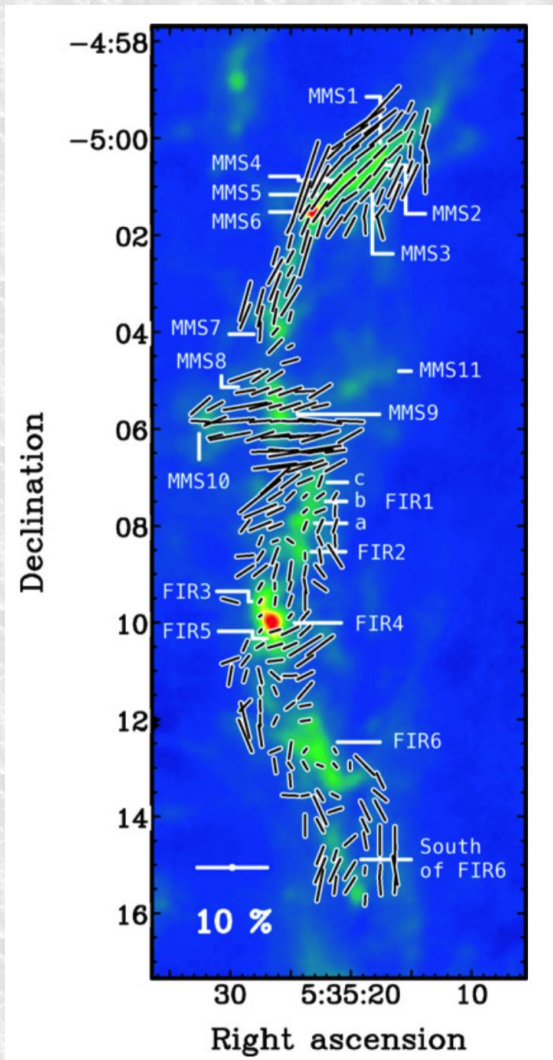
Possibly interesting points to address with NIKA2 260 polarization maps of hubs of filaments in molecular clouds:

- 1 – Angular dispersion function: is there a loss of dispersion at the typical scale of about 0.1 pc? Can we say anything about the turbulent state inside the filaments?
- 2 – HROs: do we see a change of orientation of B fields from outside to inside such hubs of filaments?
- 3 – Polarization-Intensity gradient relation: Do we see a specific change of regime in 'fragmented' regions where the gravity field dominates (virial mass).
- 4 – Multi  $\lambda$  maps: regions of interests (e.g. IC 5146, Rho Oph) have been observed with POL2 the data from which could be combined with NIKA2 for polarization spectra studies and probes of effects of radiation fields on grain alignment efficiencies.
- 5 – The method presented by **J.F. Robitaille** could also be applied to such regions and the results compared with those obtained with the other methods.





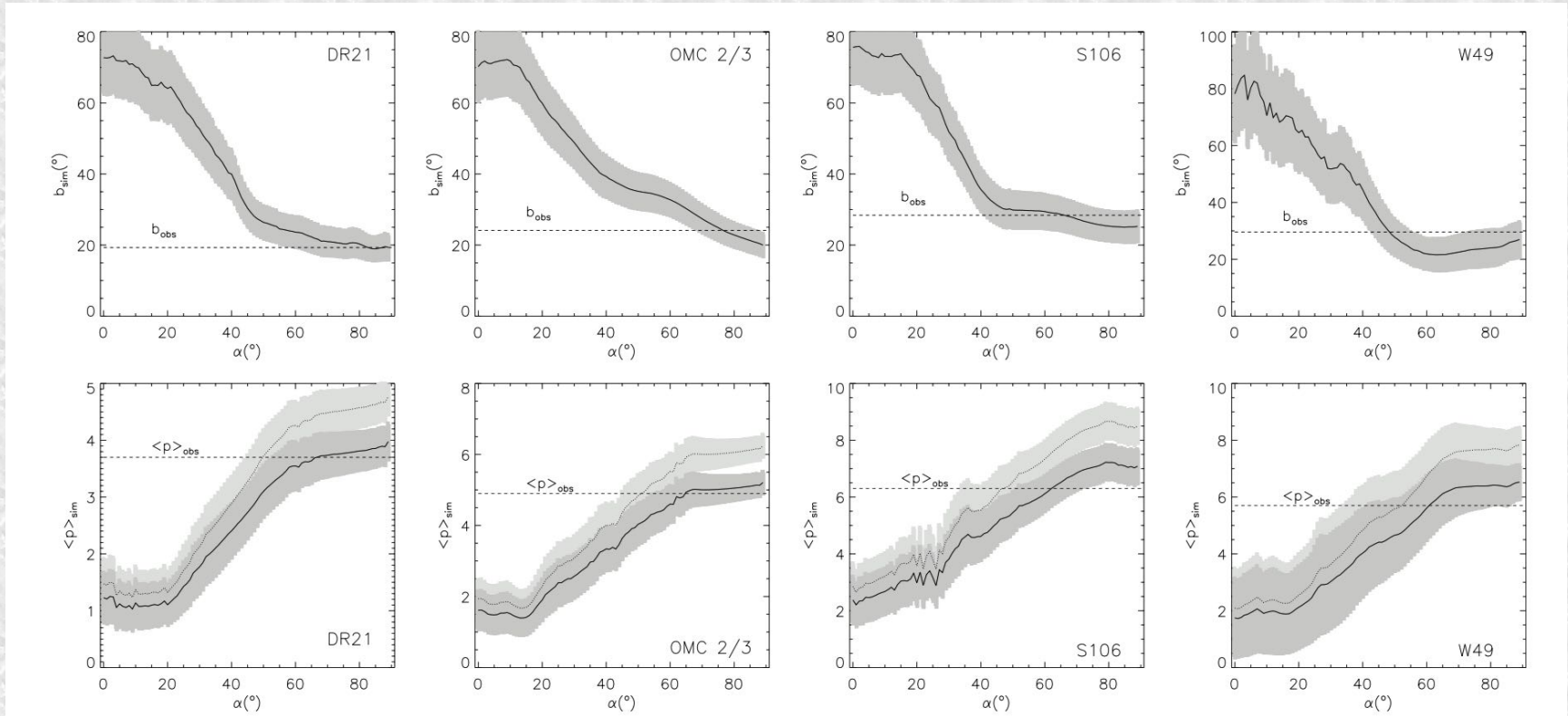
# 6) Polarimetry of dust grains as a probe of Magnetic Fields in the diffuse and dense ISM



From the analysis of such maps it is possible:

- to check on the **impact of outflows and jets on magnetic field structures**
- to **derive a 3D model of the magnetic field** by combining polarimetry by emission and absorption data sets
- to **study the impact of mag. Field on core structures** and look for correlation between star-forming cores and magnetic fields structure

## 2) Chandrasekhar & Fermi (CF) method and Angular Dispersion Function



Poidevin et al. 2013: comparison of data with MHD models → possibility to retrieve average angle of uniform 'large' scale magnetic field component with respect to line of sight.